NOT FOR PUBLICATION

NEANDC(J)-140/U
INDC(JPN)-127/U

PROGRESS REPORT

(JULY 1988 TO JUNE 1989 INCLUSIVE)

AUGUST 1989

EDITOR
S. KIKUCHI
JAPANESE NUCLEAR DATA COMMITTEE

JAPAN ATOMIC ENERGY RESEARCH INSTITUTE
TOKAI RESEARCH ESTABLISHMENT
TOKAI-MURA, IBARAKI-KEN, JAPAN

Editor's Note

This is a collection of reports which have been submitted to the Japanese Nuclear Data Committee at the committee's request. The request was addressed to the following individuals who might represent or be in touch with groups doing researches related to the nuclear data of interest to the development of the nuclear energy program.

Although the editor tried not to miss any appropriate addressees, there may have been some oversight. Meanwhile, contribution of a report rested with discretion of its author. The coverage of this document, therefore, may not be uniform over the related field or research.

In this progress report, each individual report is generally reproduced as it was received by the JNDC secretariat, and editor also let pass some simple obvious errors in the manuscripts if any.

This edition covers a period of July 1, 1988 to June 30, 1989. The information herein contained is of a nature of "Private Communication". Data contained in this report should not be quoted without the author's permission.

ELEMENT		QUANTITY	ENERGY		LAB	TYPE	DOCUMENTATION				COMMENTS
S	A		MIN	MAX			REF	VOL	PAGE	DATE	
H	PLE	N EMISSION	1.4+7		TOH	EXPT-PROG	NEANDC(J)-140			AUG 89	MATSUYAMA+.P88.TOF SPEC IN FIG
HE	4	(GAMMA,N)	2.4+7	1.0+8	TOH	EXPT-PROG	NEANDC(J)-140			AUG 89	BATES+.P103.TAGGED PHOTON SOURCE,NDG
LI	6	(N,D)	1.4+7		YOK	EXPT-PROG	NEANDC(J)-140			AUG 89	SHIRATO+.P77.PUB AS JAERI-M 80-107
LI	6	(N,T)	1.4+7		YOK	EXPT-PROG	NEANDC(J)-140			AUG 89	SHIRATO+.P77.PUB AS JAERI-M 80-107
LI	7	(N,D)	1.4+7		YOK	EXPT-PROG	NEANDC(J)-140			AUG 89	SHIRATO+.P77.PUB AS JAERI-M 80-107
LI	7	(N,T)	1.4+7		YOK	EXPT-PROG	NEANDC(J)-140			AUG 89	SHIRATO+.P77.PUB AS JAERI-M 80-107
C	12	DIFF ELASTIC	2.8+7		JAE	EXPT-PROG	NEANDC(J)-140			AUG 89	YAMANOUTI+.P14.TANDEM.CFD CC CAL,NDG
C	12	DIFF INELAST	2.8+7		JAE	EXPT-PROG	NEANDC(J)-140			AUG 89	YAMANOUTI+.P14.4.44,9.64MEV LVLS,NDG
C	12	(N,2N)	TR	4.0+7	TOH	EXPT-PROG	NEANDC(J)-140			AUG 89	NAKAMURA+.P90.ACT SIG IN FIG
N	14	(N,2N)	1.3+7	1.5+7	NAG	EXPT-PROG	NEANDC(J)-140			AUG 89	KATOH+.P73.PUB JAERI-M 89-026,P293
MG	24	SPECT (N,G)	8.4+4	4.3+5	TIT	EXPT-PROG	NEANDC(J)-140			AUG 89	UCHIYAMA+.P107.NAI(TL) DETECTOR,NDG
MG	24	RESON PARAMS	8.4+4	4.3+5	TIT	EXPT-PROG	NEANDC(J)-140			AUG 89	UCHIYAMA+P107.P-WAVE RES,PART WG,NDG
MG	26	(N,ALPHA)	1.3+7	1.5+7	NAG	EXPT-PROG	NEANDC(J)-140			AUG 89	KATOH+.P73.PUB JAERI-M 89-026,P293
AL	27	NONELA GAMMA	1.0+7	1.2+7	JAE	EXPT-PROG	NEANDC(J)-140			AUG 89	MIZUMOTO+.P16.D-D AND B11-H N, NDG
AL	27	(N,P)	1.3+7	1.5+7	NAG	EXPT-PROG	NEANDC(J)-140			AUG 89	KATOH+.P73.PUB JAERI-M 89-026,P293
AL	27	(N,ALPHA)	TR	4.0+7	TOH	EXPT-PROG	NEANDC(J)-140			AUG 89	NAKAMURA+.P90.ACT SIG IN FIG
SI		NONELA GAMMA	1.0+7	1.2+7	JAE	EXPT-PROG	NEANDC(J)-140			AUG 89	MIZUMOTO+.P16.D-D AND B11-H N, NDG
SI		(N,XN) X>2	TR	4.0+7	TOH	EXPT-PROG	NEANDC(J)-140			AUG 89	NAKAMURA+.P90.AL-28 ACT SIG IN FIG
SI	28	(N,P)	1.3+7	1.5+7	NAG	EXPT-PROG	NEANDC(J)-140			AUG 89	KATOH+.P73.PUB JAERI-M 89-026,P293
SI	30	(N,NP)	1.3+7	1.5+7	NAG	EXPT-PROG	NEANDC(J)-140			AUG 89	KATOH+.P73.PUB JAERI-M 89-026,P293

ELEMENT S	A	QUANTITY	ENERGY MIN	MAX	LAB	TYPE	DOCUMENTATION REF VOL PAGE	DATE	COMMENTS
SI	30	(N,ALPHA)	1.3+7	1.5+7	NAG	EXPT-PROG	NEANDC(J)-140	AUG 89	KATOH+.P73.PUB JAERI-M 89-026,P293
P	31	(N,2N)	1.3+7	1.5+7	NAG	EXPT-PROG	NEANDC(J)-140	AUG 89	KATOH+.P73.PUB JAERI-M 89-026,P293
P	31	(N,ALPHA)	1.3+7	1.5+7	NAG	EXPT-PROG	NEANDC(J)-140	AUG 89	KATOH+.P73.PUB JAERI-M 89-026,P293
CL	37	(N,P)	1.3+7	1.5+7	NAG	EXPT-PROG	NEANDC(J)-140	AUG 89	KATOH+.P73.PUB JAERI-M 89-026,P293
V	51	(N,P)	1.3+7	1.5+7	NAG	EXPT-PROG	NEANDC(J)-140	AUG 89	KATOH+.P73.PUB JAERI-M 89-026,P293
CR	52	(N,P)	1.3+7	1.5+7	NAG	EXPT-PROG	NEANDC(J)-140	AUG 89	KATOH+.P73.PUB JAERI-M 89-026,P293
CR	53	(N,P)	1.3+7	1.5+7	NAG	EXPT-PROG	NEANDC(J)-140	AUG 89	KATOH+.P73.PUB JAERI-M 89-026,P293
CR	53	(N,NP)	1.3+7	1.5+7	NAG	EXPT-PROG	NEANDC(J)-140	AUG 89	KATOH+.P73.PUB JAERI-M 89-026,P293
MN	55	(N,ALPHA)	1.3+7	1.5+7	NAG	EXPT-PROG	NEANDC(J)-140	AUG 89	KATOH+.P73.PUB JAERI-M 89-026,P293
FE		NONELA GAMMA	1.0+7	1.2+7	JAE	EXPT-PROG	NEANDC(J)-140	AUG 89	MIZUMOTO+.P16.D-D AND B11-H N, NDG
FE	54	(N,2N)	1.3+7	1.5+7	NAG	EXPT-PROG	NEANDC(J)-140	AUG 89	KATOH+.P73.PUB JAERI-M 89-026,P293
NI	62	(N,P)	1.3+7	1.5+7	NAG	EXPT-PROG	NEANDC(J)-140	AUG 89	KATOH+.P73.PUB JAERI-M 89-026,P293
CU	63	(N,2N)	1.3+7	1.5+7	NAG	EXPT-PROG	NEANDC(J)-140	AUG 89	KATOH+.P73.PUB JAERI-M 89-026,P293
CU	65	(N,ALPHA)	1.3+7	1.5+7	NAG	EXPT-PROG	NEANDC(J)-140	AUG 89	KATOH+.P73.PUB JAERI-M 89-026,P293
ZN		(N,XN) X>2	TR	4.0+7	TOH	EXPT-PROG	NEANDC(J)-140	AUG 89	NAKAMURA+.P90.CU-64 ACT SIG IN FIG
ZN	66	(N,P)	1.3+7	1.5+7	NAG	EXPT-PROG	NEANDC(J)-140	AUG 89	KATOH+.P73.PUB JAERI-M 89-026,P293
ZN	67	(N,NP)	1.3+7	1.5+7	NAG	EXPT-PROG	NEANDC(J)-140	AUG 89	KATOH+.P73.PUB JAERI-M 89-026,P293
ZN	68	(N,P)	1.3+7	1.5+7	NAG	EXPT-PROG	NEANDC(J)-140	AUG 89	KATOH+.P73.PUB JAERI-M 89-026,P293
SR	88	(N,P)	1.3+7	1.5+7	NAG	EXPT-PROG	NEANDC(J)-140	AUG 89	KATOH+.P73.PUB JAERI-M 89-026,P293
ZR	90	(N,2N)	1.3+7	1.5+7	NAG	EXPT-PROG	NEANDC(J)-140	AUG 89	KATOH+.P73.PUB JAERI-M 89-026,P293

ELEMENT S	A	QUANTITY	ENERGY MIN	MAX	LAB	TYPE	DOCUMENTATION REF	VOL	PAGE	DATE	COMMENTS
ZR	94	(N,P)	1.3+7	1.5+7	NAG	EXPT-PROG	NEANDC(J)-140			AUG 89	KATOH+.P73.PUB JAERI-M 89-026,P293
NB	93	N EMISSION	1.4+7		KYU	THEO-PROG	NEANDC(J)-140			AUG 89	WATANABE+.P65.2-COMP EXCITON MDL,NDG
MO	92	(N,2N)	1.3+7	1.5+7	NAG	EXPT-PROG	NEANDC(J)-140			AUG 89	KATOH+.P73.PUB JAERI-M 89-026,P293
MO	92	(N,ALPHA)	1.3+7	1.5+7	NAG	EXPT-PROG	NEANDC(J)-140			AUG 89	KATOH+.P73.PUB JAERI-M 89-026,P293
MO	97	(N,P)	1.3+7	1.5+7	NAG	EXPT-PROG	NEANDC(J)-140			AUG 89	KATOH+.P73.PUB JAERI-M 89-026,P293
MO	98	(N,NP)	1.3+7	1.5+7	NAG	EXPT-PROG	NEANDC(J)-140			AUG 89	KATOH+.P73.PUB JAERI-M 89-026,P293
IN	113	(N,2N)	1.3+7	1.5+7	NAG	EXPT-PROG	NEANDC(J)-140			AUG 89	KATOH+.P73.PUB JAERI-M 89-026,P293
IN	115	N EMISSION	1.4+7		KYU	THEO-PROG	NEANDC(J)-140			AUG 89	WATANABE+.P65.2-COMP EXCITON MDL,NDG
SN	122	RESON PARAMS	1.5+3	3.0+4	JAE	EXPT-PROG	NEANDC(J)-140			AUG 89	NAKAJIMA+.P17.TRANS,21RES,D=1.17KEV
SN	122	STRNTH FNCTN	1.5+3	3.0+4	JAE	EXPT-PROG	NEANDC(J)-140			AUG 89	NAKAJIMA+.P17.S0=(0.30+0.12-0.08)E-4
SB		TOTAL	1.0-2	3.0+6	KTO	EXPT-PROG	NEANDC(J)-140			AUG 89	KOBAYASHI+.P42.LINAC,CFD OTH IN FIGS
SB		(N,GAMMA)	NDG		KTO	EXPT-PROG	NEANDC(J)-140			AUG 89	YAMAMOTO+.P54.BGO DET, IN PROGRESS
GD	155	(N,GAMMA)	1.1+3	2.4+5	JAE	EXPT-PROG	NEANDC(J)-140			AUG 89	NAKAJIMA+.P15.TBP IN ANN.NUCL.ENERGY
GD	155	RESON PARAMS	1.1+3	2.4+5	JAE	EXPT-PROG	NEANDC(J)-140			AUG 89	NAKAJIMA+.P15.TBP IN ANN.NUCL.ENERGY
GD	155	STRNTH FNCTN	1.1+3	2.4+5	JAE	EXPT-PROG	NEANDC(J)-140			AUG 89	NAKAJIMA+.P15.TBP IN ANN.NUCL.ENERGY
GD	157	(N,GAMMA)	1.1+3	2.4+5	JAE	EXPT-PROG	NEANDC(J)-140			AUG 89	NAKAJIMA+.P15.TBP IN ANN.NUCL.ENERGY
GD	157	RESON PARAMS	1.1+3	2.4+5	JAE	EXPT-PROG	NEANDC(J)-140			AUG 89	NAKAJIMA+.P15.TBP IN ANN.NUCL.ENERGY
GD	157	STRNTH FNCTN	1.1+3	2.4+5	JAE	EXPT-PROG	NEANDC(J)-140			AUG 89	NAKAJIMA+.P15.TBP IN ANN.NUCL.ENERGY
AU	197	(N,GAMMA)	NDG		KTO	EXPT-PROG	NEANDC(J)-140			AUG 89	YAMAMOTO+.P54.BGO DET, IN PROGRESS
PB		NONELA GAMMA	1.0+7	1.2+7	JAE	EXPT-PROG	NEANDC(J)-140			AUG 89	MIZUMOTO+.P16.D-D AND B11-H N, NDG

ELEMENT S	A	QUANTITY	ENERGY MIN	MAX	LAB	TYPE	DOCUMENTATION REF	VOL	PAGE	DATE	COMMENTS
BI	209	NONELA GAMMA	1.0+7	1.2+7	JAE	EXPT-PROG	NEANDC(J)-140			AUG 89	MIZUMOTO+.P16.D-D AND B11-H N, NDG
TH	232	N EMISSION	1.2+6	1.4+7	TOH	EXPT-PROG	NEANDC(J)-140			AUG 89	BABA+.P86.PUB IN JAERI-M 89-026,P253
U	232	EVALUATION	NDG		KNK	EVAL-PROG	NEANDC(J)-140			AUG 89	OHSAWA+.P29.FOR JENDL-3, NDG
U	235	SPECT FISS N	NDG		KNK	REVW-PROG	NEANDC(J)-140			AUG 89	OHSAWA.P31.PUB JAERI-M 89-026,P114
U	235	SPECT FISS N	NDG		KYU	EVAL-PROG	NEANDC(J)-140			AUG 89	KAWANO+.P69.PUB JAERI-M 89-026,P275
U	238	TOT INELAST	NDG		KYU	EVAL-PROG	NEANDC(J)-140			AUG 89	UENOHARA+.P68.STAT+CC MDL CALC, NDG
U	238	DIFF INELAST	NDG		KYU	EVAL-PROG	NEANDC(J)-140			AUG 89	UENOHARA+.P68.STAT+CC MDL CALC, NDG
U	238	N EMISSION	1.2+6	1.4+7	TOH	EXPT-PROG	NEANDC(J)-140			AUG 89	BABA+.P86.PUB IN JAERI-M 89-026,P253
U	238	SPECT FISS N	2.0+6		TOH	EXPT-PROG	NEANDC(J)-140			AUG 89	BABA+.P83.PUB IN JAERI-M 89-026,P253
AM	241	EVALUATION	NDG		JAE	EVAL-PROG	NEANDC(J)-140			AUG 89	NAKAGAWA.P20.PUBL AS JAERI-M 89-008
AM	242	EVALUATION	NDG		JAE	EVAL-PROG	NEANDC(J)-140			AUG 89	NAKAGAWA.P20.PUBL AS JAERI-M 89-008
AM	243	EVALUATION	NDG		JAE	EVAL-PROG	NEANDC(J)-140			AUG 89	NAKAGAWA.P20.PUBL AS JAERI-M 89-008
AM	244	EVALUATION	NDG		JAE	EVAL-PROG	NEANDC(J)-140			AUG 89	NAKAGAWA.P20.PUBL AS JAERI-M 89-008
CF	252	SPECT FISS N	SPON		KYU	EVAL-PROG	NEANDC(J)-140			AUG 89	KAWANO+.P69.PUB JAERI-M 89-026,P275
MANY		DIFF INELAST	1.4+7		KYU	THEO-PROG	NEANDC(J)-140			AUG 89	KUMABE+.P61.TBP IN NUCL. SCI. ENG.
MANY		DIFF INELAST	FISS		KNK	EXPT-PROG	NEANDC(J)-140			AUG 89	HORIBE+.P32.ACT SIG/REL AL27NA.NDG
MANY		(N,2N)	FISS		KNK	EXPT-PROG	NEANDC(J)-140			AUG 89	HORIBE+.P32.ACT SIG/REL AL27NA.NDG
MANY		N EMISSION	1.4+7	2.6+7	KYU	THEO-PROG	NEANDC(J)-140			AUG 89	WATANABE+.P62.PUB JAERI-M89-026,P300
MANY		(N,P)	1.4+7		KYU	THEO-PROG	NEANDC(J)-140			AUG 89	KUMABE+.P61.TBP IN NUCL. SCI. ENG.
MANY		(N,P)	FISS		KNK	EXPT-PROG	NEANDC(J)-140			AUG 89	HORIBE+.P32.ACT SIG/REL AL27NA.NDG

ELEMENT S A	QUANTITY	ENERGY MIN	ENERGY MAX	LAB	TYPE	DOCUMENTATION REF VOL PAGE	DATE	COMMENTS
MANY	(N,ALPHA)	1.4+7		KYU	THEO-PROG	NEANDC(J)-140	AUG 89	KUMABE+.P61.TBP IN NUCL. SCI. ENG.
MANY	(N,ALPHA)	FISS		KNK	EXPT-PROG	NEANDC(J)-140	AUG 89	HORIBE+.P32.ACT SIG/REL AL27NA.NDG
MANY	FISSION	NDG		KNK	THEO-PROG	NEANDC(J)-140	AUG 89	OHSAWA.P30.PUB IAEA-TECDOC-483/P134

The content table in the CINDA format was compiled by the JNDC CINDA group;

M. Kawai (NAIG), H. Kitazawa (Tokyo Inst. of Tech.),
T. Nakagawa (JAERI), R. Nakasima (Hosei Univ.),
M. Sakamoto (JAERI), K. Shibata (JAERI).

I. ELECTROTECHNICAL LABORATORY

A. Radiation Metrology Section

I-A-1 Emission Probability of 46.5 keV γ-Ray of Pb-210

Y. Hino and Y. Kawada

Pb-210 is also known by the historical name of RaD and is often used as an alpha- and/or beta-ray standard source, since the daughter nuclide ^{210}Bi(RaE) emits pure beta-rays with the maximum energy of 1.16 MeV and the grand-daughter nuclide ^{210}Po(RaF) emits 5.3 MeV alpha-particles. The ^{210}Pb itself emits very soft beta rays with about 80% of the decay populating the 46.5 keV excited state of ^{210}Bi. The gamma transition from the excited state is, however, highly internally converted to L-electrons so that the gamma-ray emission probability is only a few percent. In the decay chain of ^{210}Pb(RaD)-^{210}Bi(RaE)-^{210}Po(RaF)-^{206}Pb(RaG), no other gamma-rays are observed, and hence this 46.5 keV gamma-ray would be useful as a gamma-ray standard, if the γ-ray intensity per decay were known with a reasonable accuracy. The fact that the nuclide has a long half life of 22.3 years makes it especially suitable for a radioactivity standard.

So far few measurements with modern instruments have been reported on the intensity per decay of this 46.5 keV gamma-ray, except those by Debertin and Peßara[1).

In this report, an accurate determination of this emission probability was carried out by the combination of two techniques of improved 2πα counting and gamma-ray spectrometry. For the latter a high-purity germanium detector with a thin ion-implanted front contact whose response is nearly flat in the region below 100 keV was used.

The spectrometer was calibrated by using standard sources of ^{57}Co, ^{111}In, ^{139}Ce and ^{241}Am which were all standardized in our laboratory by the use of the 4πα-γ or 4πx-γ coincidence techniques. The efficiency decreases with decreasing the photon energies below 30 keV mainly due to the escape of the K-x-rays of germanium from the crystal. The loss of peak area due to this escape can be corrected by adding the area of the escape peak to the main peak area. It was found that the efficiencies corrected for the escape peak and attenuation in all materials between the source and detector are nearly constant over the energy range from 20 keV to 70 keV, which improves the reliability of the efficiency interpolation.

Four ^{210}Pb sources were used and each had a source strength around 600 Bq. The total counting time was 300,000 s for each source. The final result for the 46.5 keV gamma-ray emission probability is 0.0426 $\pm$ 0.0007 (1 σ) after the correction for the x-ray escape (1.3 %), and attenuation in the aluminum cover (0.60%), in air (0.09%) and in the dead layer of the crystal (0.06%). The present result is compared with other reported values and evaluations in Table 1. The value reported by Debertin and Peßara[1)] is in agreement with our result within the stated uncertainties, and the value in NCRP-58[2)] is related to their value. The other evaluations[6-8)] have a lower value which is based on the older result of Krause[5)]. The very recent measurement by Schotig is in compleate agreement with the present result[9)].

This wok was presented in the International Symposium on Nuclear Decay Data: Spectrometric Methods, Measurements and Evaluations(6-8 June, 1989, at Braunschweig, Federal Republic of Germany), and will be published in NIM.

References

1) K. Debertin and W. Peßara, Int J. Appl. Radiat. Isot. 34(1983) 515
2) NCRP Report No.58 (National Council on Radiation Protection and Measurements, 1985)
3) P.E. Demon and R.R. Edwards, Phys. Rev. 95(1954) 1648
4) R.W.Fink, Phys. Rev. 106(1957) 266
5) I.V. Krause, Z. Physik 152(1958) 586
6) B. Harmatz, Nucl. Data Sheets 34(1981) 735
7) F. Lagoutine, N. Coursol and J. Legrand, Table de Radionucleides (LMRI,Saclay, 1985)
8) E. Browne and R.B. Firestone, Table of Radioactive Isotopes (Wiley-Interscience, 1986)
9) U. Schotzig, To be appeared in Nucl. Instr. and Meth.

Table 1 Comparison of the present result with other reported values and evaluations.

Author/Ref.	Method	γ emission probability
Damon et al.(1954)[3]	Thin NaI scin. spect. and α prop. counter	0.038 ± 0.006
Fink(1957)[4]	NaI scin. spect. and α prop. counter	0.045 ± 0.004
Krause(1958)[5]	NaI scin. spect. and ZnS scin. counter	0.0405 ± 0.0008
Debertin & Peßara(1981)[1]	Ge spect.	0.0418 ± 0.0008
Nucl. Data Sheet(1981)[6]	Evaluation	0.0405 ± 0.0008
Lagoutine et al.(1985)[7]	Evaluation	0.0406 ± 0.0008
Table of Radioactive Tables(1986)[8]	Evaluation	0.0405 ± 0.0020
NCRP Report No.58(1985)[2]	Evaluation	0.0418 ± 0.0023
Present work	See text	0.0426 ± 0.0007

Add in proof: U. Schotzig; 0.0424 ± 0.0006 [9]

I-A-2

Decay Data of Tl-201

Y.Kawada and Y.Hino

Thallium-201 is an important radionuclide in the field of nuclear medicine. Routine quantitative measurements are often performed using a pressurized ionization chamber. However, inevitably this radionuclide contains ^{200}Tl, ^{202}Tl and other radioactive impurities, which may cause the response of the calibrating instrument to be considerably overestimated because of an abundance of high-energy gamma-rays emitted by these impurities. Gamma-ray spectroscopy offers an alternative method of analyses, free from the influence of such impurities, to give greater reliability, if the gamma- and x-ray emission probabilities are known with reasonable accuracy.

The decay parameters have been reported by Debertin et al.[1], Funck et al.[2] and Nass[3], but discrepancies of between 5 to 10% can be found between these measurements and evaluations[4-7]. The measurements by Debertin et al.[1] was based upon the measurements of relative gamma- and x-ray emission probabilities of ^{201}Tl, and the absolute data were derived by the normalisation against the K_α x-ray peak. Therefore, any significant uncertainty in the K_α x-ray emission probability will have a large impact on the derivation of the other gamma- and x-ray emission probabilities. Funck et al.[2] determined the absolute emission probabilities per decay of gamma- and x-rays by using photon spectrometers to measure the photon emission rates and the $4\pi\beta$-γ coincidence technique to measure the radioactivity. However, considerable discrepancies are found between these two sets of measurements; there is about 3.5% difference between the reported emission probabilities for the 167 keV gamma-ray.

Efforts have been made to measure the gamma- and x-ray emission probabilities per decay with improved accuracy in this study. An advanced photon detector system and the technique of the $4\pi\beta$-γ efficiency extrapolation taking into account the influence of the summing effects of the K x-rays and gamma-rays have been used to these measurements.

The radioactivity measdurements were carried out by a $4\pi e$-x coincidence extrapolation technique with a conventional $4\pi x$-γ coincidence system was used with two 7.6 x 7.6 cm NaI(Tl) crystals for gamma-ray detector. A cadmium sheet with a thickness of 0.5mm was inserted between the $4\pi\beta$ counter and each of the gamma-ray detectors so that coincidence summing was diminished[8].

The gamma-gate covered the 167 keV peak, and the one-dimensional efficiency extrapolation was applied to the data to determine the absolute activity. Counting efficiencies in the β-channel were varied by adjusting the solid content of the carrier material, and/or the sources were covered with additional gold-coated VYNS foils. A pressurized $4\pi\beta$ counter (1 MPa) was also used to improve the detection efficiencies in the beta-channel. These measurements exhibit a linear relationship over a wide range of $(1 - \varepsilon_\beta)/\varepsilon_\beta$ with Cd absorbers as compared with experiments without Cd absorbers. The slopes of the two lines differ significantly, while extrapolation to a zero value for $(1 - \varepsilon_\beta)/\varepsilon_\beta$ resulted in a difference of approximately 1.5%. Furthermore the data obtained without Cd absorber were very sensitive to other experimental conditions such as the detector-source geometry.

A highly purity coaxial Ge detector (reverse-electrode closed-end coaxial detector LO-AX type(EG&G Ortec)) was used for the photon measurements. A thin inactive layer(less than 0.3 μm) and a beryllium window(0.5 mm thick) ensure a nearly flat response in the energy range from several to 100 keV. The Ge crystal had a active region of 35.7 x 13.3 mm^2, and gave an energy resolution(FWHM) of 270eV at 5.9keV and 540eV at 122keV. The source-detector distance was always maintained at 20cm, and the detector was shielded with 6 cm thick lead lined with 5 cm steel, 5 mm copper and 5 mm Perspex. A Seiko-EG&G 7800 multichannel analyser was used with a total memory of 2 x 4K.

The spectrometer was calibrated with the standard point sources of ^{57}Co, ^{111}In, ^{139}Ce and ^{241}Am. These sources were all standardised in our laboratory by the use of the $4\pi\alpha$-γ or $4\pi x$-γ coincidence techniques.

Seven sources were used to measure the photon emission probabilities, and each source strength was approximately 30,000 Bq. The emission probability per decay of each gamma- and x-ray was determined from the area, calibrated efficiency and source activity, after making corrections for the escape peak and absorption in the aluminum cover, air, and the inactive layer of the detector. The results are listed in Table 1 together with other reported data and evaluations. The new measurements differ significantly from earlier studies; the emission probability of the 167 keV gamma-ray is 8% lower than the measurements of Debertin et al.[1], and 4% lower than reported by Funck[2], and 2% lower than the studies of Nass[3]. Some of published evaluations[5,7] are based on the data of Debertin et al.[1], and are inconsistent with the present results. These significant disagreement warrant more extensive studies of the decay data of ^{201}Tl on an international basis.

This work was presented in the International Symposium on Nuclear decay Data: Spectrometric Methods, Measurements and Evaluations(6-8 June, 1989 at Braunschweig, Federal republic of Germany), and will be published in NIM.

References

1) K.Debertin, W.Pessara, U.Schotzig and K.F.Walz, Int. J. Appl. Radiat. Isotop. 30(1979)551
2) E.Funck, K.Debertin and K.F.Walz, Int. J. Nucl. Med. Biol. 10(1983) 137
3) H.W.Nass, J. Nucl. Med. 18(1977)
4) National Committee for Radiological Protechtion, NCRP Report No.58, 2nd Ed.(NCRP, 1985)
5) F.Lagoutine, N.Coursol and J.Legrand, Table de Radionucleides(LMRI, Saclay, 1984)
6) M.R.Schmorak, Nuclear Data Sheets 49(1986)733
7) E.Browne and R.B.Firestone, Table of Radioactive Isotopes(Wiley -Interscience, 1986)
8) E.Funck, Appl. Radiat. Isot., Int. J. Radiat. Appl. Instrum. Part A 38(1987)771

Table 1 Photon emission probabilities per decay of ^{201}Tl

Energy (keV)	This work	Debertin et al.[1]	Funck et al.[2]	Nass[3]	NCRP-58[4]	Table de Radionucleide[5]	NDS[8]	Table of Radioactive Isot.[7]
30.6	0.00255(8)	0.00272(13)	0.00267(8)	0.00310(13)	0.00272(13)	0.0027(1)	0.00272(7)	0.0022(2)
32.2	0.00267(6)	0.00276(15)	0.00267(7)	0.00285(12)	0.00276(15)	0.0027(1)	0.00276(9)	0.0022(2)
68.9($K_{\alpha2}$)	0.265(4)				0.277(10)	0.274(8)	–	0.269(24)
		0.750(35)	0.740(13)	0.740(23)				
70.8($K_{\alpha1}$)	0.434(6)				0.472(16)	0.466(12)	–	0.46(4)
80.2–82.5(K_{β})	0.191(5)	0.211(10)	0.210(4)	0.205(7)	0.208(8)	0.210(4)	–	0.205(18)
135.3	0.0267(5)	0.0280(11)	0.0272(4)	0.0265(10)	0.0280(11)	0.0270(10)	0.0280(3)	0.0267(13)
165.9	0.00142(20)	0.0016(2)	0.0015(2)	0.0018(2)	0.0016(2)	0.0016(1)	0.00166(10)	0.0016(1)
167.4	0.0981(12)	0.1060(42)	0.1025(10)	0.1000(17)	0.106(5)	0.1025(20)	0.106(5)	0.094(11)

II. Japan Atomic Energy Research Institute

A. Linac Laboratory

Department of Physics

II-A-1 The $^{1}H(^{11}B,n)^{11}C$ Reaction As A Practical Low Background Monoenergetic Neutron Source In The 10 MeV Region

S. Chiba, M. Mizumoto, K. Hasegawa*, Y. Yamanouti, M. Sugimoto, Y. Watanabe** and M. Drosg***

A paper on this subject will be published in Nucl. Instr. Methods. A. (1989) with an abstract as follows:

Neutron source properties of the $^{1}H(^{11}B,n)^{11}C$ reaction were measured for incident ^{11}B energies between 50 and 64 MeV by detecting the neutrons at angles of 0° to 40°. Neutrons were produced with high monochromaticity in the range of several MeV to 12 MeV. In addition, the room background is very low because they were collimated to a forward cone according to the kinematical condition. Therefore, this reaction was proved to be a desirable monoenergetic neutron source in the "gap" region and was applied successfully to the neutron physics research at the JAERI tandem accelerator.

---

* On leave from Tohoku University as a research student

** University of Kyushu

*** University of Wien

II-A-2

Scattering of 28.15 MeV neutrons from ^{12}C

Y. Yamanouti, M. Sugimoto, S. Chiba, M. Mizumoto, Y. Watanabe*

and K. Hasegawa**

Differential cross sections for elastic and inelastic scattering (4.439 MeV 2^+, 9.641 MeV 3^-) on ^{12}C were measured at an incident energy of 28.15 MeV in order to study the reaction mechanism for the neutron scattering in the energy region around 30 MeV and the collective nature of ^{12}C.

A pulsed beam of protons was provided by the tandem accelerator. Neutrons were generated by the $^7Li(p,n)^7Be$ reaction. An array of four 20 cm in diam by 35 cm thick NE213 liquid scintillator detectors was used for neutron measurements. The differential cross sections were normalized to the known n-p scattering differential cross sections by measuring neutrons scattered from a polyethylene scatterer.

These experimental data were analyzed by the optical model and the coupled-channel theory, and compared with proton scattering in the framework of the Lane model. The rotational model calculation with the oblate quadrupole and hexadecapole deformation gives good fit to the experimental cross sections for the elastic and inelastic scattering on ^{12}C.

---

* Department of Nuclear Engineering, Kyushu University

** Department of Nuclear Engineering, Tohoku University

II-A-3

Neutron capture cross section measuremetns of ^{155}Gd and ^{157}Gd from 1.1 to 235 keV

Yutaka NAKAJIMA, Izumi TSUBONE[+], Motoharu MIZUMOTO, Yutaka FURUTA, Makio OHKUBO, Masayoshi SUGIMOTO and Yuuki KAWARASAKI

A paper on this subject will be published in Annals of Nuclear Energy with the following abstract:

Neutron capture cross section measurements of ^{155}Gd and ^{157}Gd were made at the Japan Atomic Energy Research Institute linac in the energy range from 1.1 to 235 keV. The results were compared to other measurements and to the JENDL-2 evaluation. The analysis of the capture cross sections by the least squares method gives the following average resonance parameters:
$10^4S_0 = 3.00 \pm 0.28$, $10^4S_1 = 3.7 \pm 1.1$, $< \Gamma_\gamma{}^s > = 119 \pm 29$ eV, $< \Gamma_\gamma{}^p > = 140 \pm 60$ eV for ^{155}Gd, and $10^4S_0 = 2.23 \pm 0.57$, $10^4S_1 = 2.2 \pm 0.7$, $< \Gamma_\gamma{}^s > = 115 \pm 28$ eV, $< \Gamma_\gamma{}^p > = 129 \pm 25$ eV for ^{157}Gd.

[+] On leave from Kyushu University as a research student in the Japan Atomic Energy Research Institute.
Present address: Design Division of Nuclear Instrumentation, Tokyo Factory, Fuji Electric Co., Ltd., Fuji-machi, Hino-shi 191, Japan.

II-A-4 Gamma-ray Production Cross Sections of Al, Si, Fe, Pb and Bi

M. Mizumoto, K. Hasegawa*, S. Chiba, M. Sugimoto, Y. Yamanouti, M. Igashira**, T. Uchiyama** and H. Kitazawa**

We have been continuing to measure neutron induced γ -ray production cross sections for last several years at the JAERI Tandem Accelerator. We have extended the data for structural and shielding materials such as Al, Si, Fe, Pb and Bi to 10 and 11.5 MeV using neutron sources by the $^{2}H(d,n)^{3}He$ and the $^{1}H(^{11}B,n)^{11}C$ reaction, respectively. Emitted γ -rays were measured with a 7.6cmϕ x 15cm NaI(Tl) detector surrounded by an 25.4cmϕ x 25.4cm annular NaI(Tl) detector. The raw data of gamma-ray spectra were unfolded with the computer program FERDOR. The response functions of the γ -ray detector were determined with the γ -rays from the standard sources and several discrete γ -rays from the 992 keV resonances of $^{27}Al(p,\gamma)$ and 935 keV resonance of $^{19}F(p,\gamma)$. The measured results were compared with existing data by the continuous neutron source at ORELA and with the new evaluated data JENDL-3 based on the multi-step Hauser Feshbach calculation.

---

* On leave from Tohoku University as a research student
** Tokyo Institute of Technology

II-A-5

Measurements of resonance parameters of ^{122}Sn

Yutaka NAKAJIMA, Makio OHKUBO, Yutaka FURUTA, Motoharu MIZUMOTO,

Masayoshi SUGIMOTO, and Yuuki KAWARASAKI

A paper on this subject will be submitted to Annals of Nuclear Energy with the following abstract:

Neutron transmission measurements were carried out on an ^{122}Sn oxide sample enriched to 92.20 % at a 190-m station with the neutron time-of-flight method. Resonance energies and neutron widths were determined for 21 resonances between 1.5 and 30 keV by a shape analysis code based on the Breit-Wigner multi-level formula. Following average resonance parameters for s-wave neutrons were obtained: $D_0 = 1.17^{+0.09}_{-0.08}$ keV, $S_0 \times 10^4 = 0.30^{+0.12}_{-0.08}$ and $R' = 5.60 \pm 0.05$ fm. The present s-wave neutron strength function of ^{122}Sn is substantially larger than the theoretical prediction of the doorway state model.

II-A-6 Detector System for Gamma-ray Production Cross Section Measurements and Data Analysis

Kazuo Hasegawa* and Motoharu Mizumoto

A paper on this subject was published in JAERI-M 89-042 (1989) with an abstract as follows:

A detector system for double-differential gamma-ray production cross section measurements has been installed in the JAERI Tandem Accelerator and data analysis computer codes have been developed. Gamma-ray pulse-height spectra have been measured by a 3" dia. x 6 " anti-Compton NaI(Tl) detector. Response matrix of the detector has been obtained and evaluated by some pulse-height spectra using standard gamma-ray sources and reaction gamma-rays such as $^{12}C(n,n'\gamma)$, $^{16}O(n,n'\gamma)$, $^{27}Al(p,\gamma)$, $^{19}F(p,\alpha\gamma)$. Gamma-ray production cross sections have been deduced by means of unfolding and normalization of neutron flux and number of sample atoms.

In this report, outline of the detector system and process of data analysis have been presented.

---

* On leave from Tohoku University as a research student

II-A-7 <u>The Influence of Water Absorption in Samples for Neutron Capture Cross Section Measurements</u>

Motoharu Mizumoto and Masayoshi Sugimoto

A paper on this subject will be published in Nucl. Instr. Methods A (1989) with an abstract as follows:

Sample-related corrections for average neutron capture cross section measurements are complicated in the keV region due to the resonance structure. In particular, light mass nuclei present in chemical compounds of rare earth materials make corrections for neutron multiple-scattering and self-shielding difficult. Moreover, samples of chemical compounds such as oxides are hygroscopic. A Monte Carlo method has been developed by taking into account the effects caused by neutron slowing down into the resonance region due to the scattering from hydrogen and oxygen atoms. The validity of the calculated corrections has been investigated by comparing experimental data of oxide and metallic samples. The calculation method and relate problems will be discussed.

B. Nuclear Data Center, Department of Physics and Working Groups pf Japanese Nuclear Data Committee

II-B-1 Evaluation of Nuclear Data for Americium Isotopes

Tsuneo NAKAGAWA

A paper on this subject was published as JAERI-M 89-008 (1989) with an abstract as follows:

The nuclear data of ^{241}Am, ^{242g}Am, ^{242m}Am and ^{243}Am, which are stored in JENDL-2, were compared with recent experimental data. New experimental data of americium isotopes except ^{242g}Am have been reported since the JENDL-2 evaluation was made. The data of these nuclides were reevaluated on the basis of the new experimental data. Mainly revised data are the fission and capture cross sections and resonance parameters. The inelastic scattering cross sections were also re-calculated by adopting new level-scheme data. The data of ^{244g}Am and ^{244m}Am, which were not stored in JENDL-2, were newly evaluated. Only available experimental data for ^{244}Am were thermal cross sections. The shape of the fission cross section was determined to be the same as that of ^{242g}Am, and other data were calculated with CASTHY.

II-B-2

Evaluation of the (α,n) Reaction Data for Light Nuclei

Hiroyuki MATSUNOBU*

The nuclear data of (α,n) reaction are earnestly required in the fields of radiation shielding and criticality safety relating to the spent fuel and high level waste including TRU. In order to prepare the required data of (α,n) reaction for light nuclei, evaluation work is in progress as a part of the activities for Post JENDL-3 Project. During the past two years, the (α,n) reaction data for the following isotopes and elements were preliminarily evaluated in the energy range from the threshold energies to 15 MeV:

^{6}Li, ^{7}Li, ^{nat}Li, ^{10}B, ^{11}B, ^{nat}B, ^{12}C, ^{13}C, ^{nat}C,

^{17}O, ^{18}O, ^{nat}O, ^{23}Na, ^{28}Si, ^{29}Si, ^{30}Si, and ^{nat}Si.

In the present work, the compiled experimental data for the total cross section of (α,n) reaction were analyzed using the ELIESE-3 code[1] based on the statistical theory and optical model. In this analysis, the optimum OMP(Optical Model Parameter) sets were searched for so as to reproduce the global shapes of the cross sections. However, it is not so easy to reproduce the global shapes over the whole energy range, because the measured data show the remarkable resonance structures. Accordingly, the cross sections in some energy intervals where the differences are large between the calculated values and measured data, were modified by following the most reliable measured data.

The neutron yields for thick targets were calculated using the evaluated (α,n) cross sections and stopping powers by Ziegler[2], and were compared with the recent measurements by Bair and Gomez del Campo[3],

* Sumitomo Atomic Energy Industries, Ltd.

West and Sherwood[4], and Jacobs and Liskien[5]. As the result of this comparison, large discrepancies were found out between the cross section and neutron yield data for boron isotoptes. At present, the cause of discrepancies is being examined on the basis of the other data.

The energy spectra of neutrons emitted from the thick targets were also calculated by the ORIGEN-JR code[6] with the angular distributions of neutrons obtained by ELIESE-3 code and the neutron yields.
The results for B, C, O, and Si were compared with the measurements by Jacobs and Liskien. However, the agreement with their data is not so well, because their data were measured in the energy range of 4.0 to 5.5 MeV where reproduction of the (α,n) cross sections is most difficult due to the remarkable resonance structures.

The preliminary results of the present evaluation are shown partially in Fig. 1 to Fig. 8.

References:

1) Igarasi, S.: Program ELIESE-3; Program for calculation of the Nuclear Cross Sections by Using Local and Non-Local Optical Models and Statistical Model, JAERI 1224 (1972)
2) Ziegler, J. F. : Helium stopping Powers and Ranges in all Elemental Matter, Pergamon Press, Oxford, (1977)
3) Bair, J. K. and Gomez del Campo, J. : Nucl. Sci. Eng., 71, 18 (1979)
4) West, D. Sherwood, A. C. : Ann. Nucl. Energy 9, 551 (1982)
5) Jacobs, G. J. H. and Liskien, H. : Ann. Nucl. Energy 10, 541 (1983)
6) Koyama, K., Yamano, N., and Miyasaka, S. : ORIGEN-JR; A Computer Code for Calculating Radiation Sources and Analyzing Nuclide Transmutations, JAERI-M 8229 (1979)

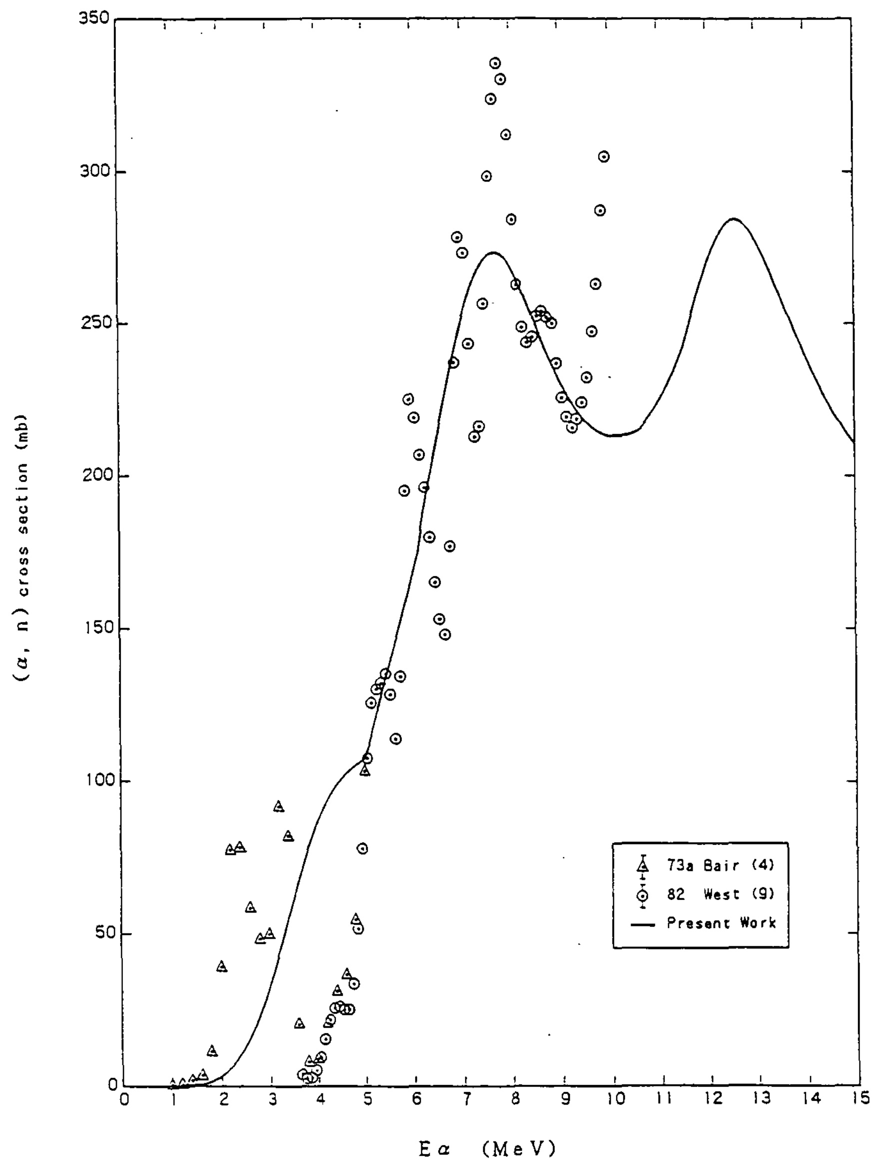

Fig. 1 (α, n) Reaction Cross Section of ^{13}C

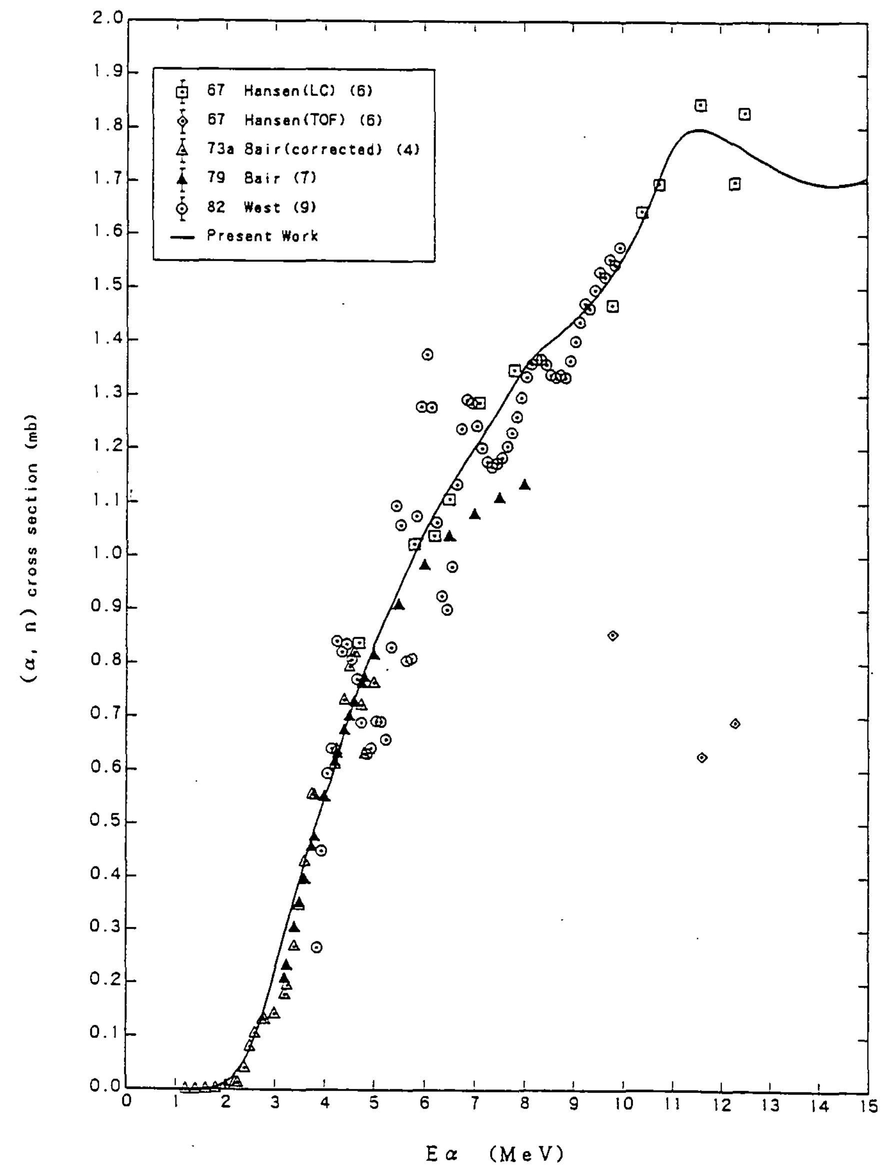

Fig. 2 (α, n) Reaction Cross Section of ^{nat}O

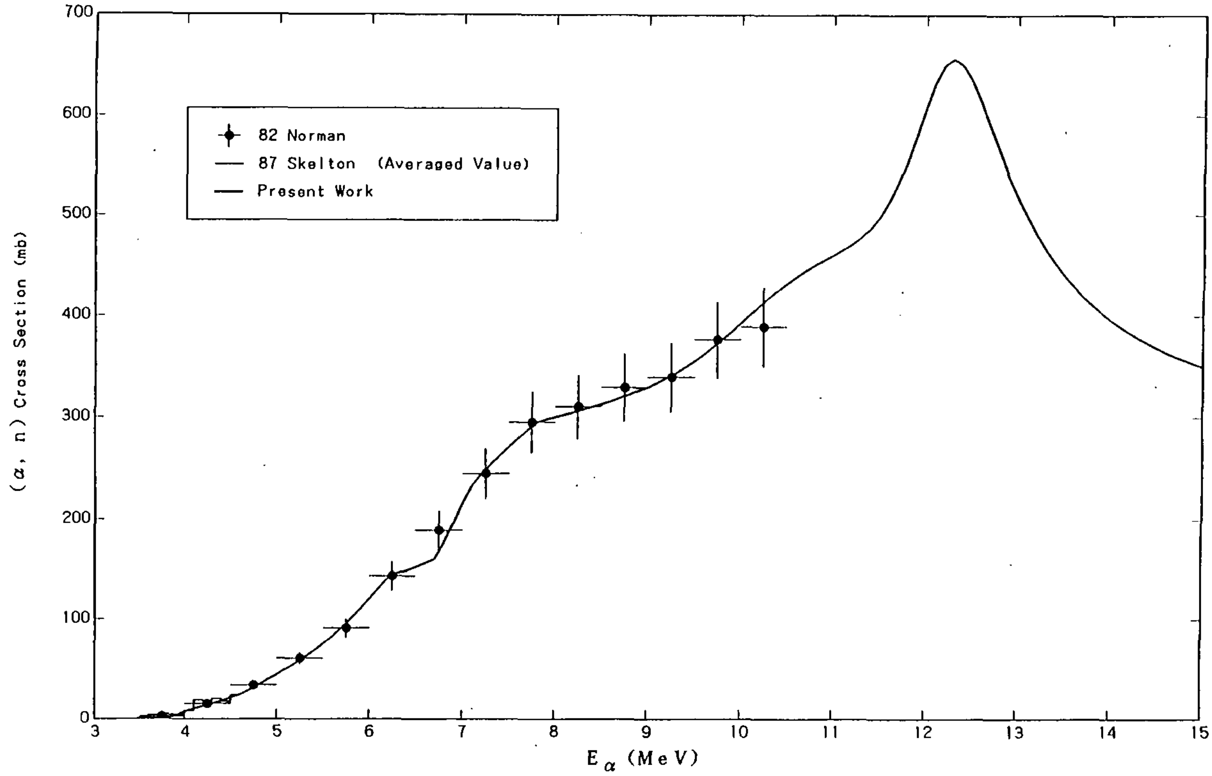

Fig. 3 ^{23}Na (α, n) ^{26}Al reaction cross sections in the energy range from 3 to 15 MeV

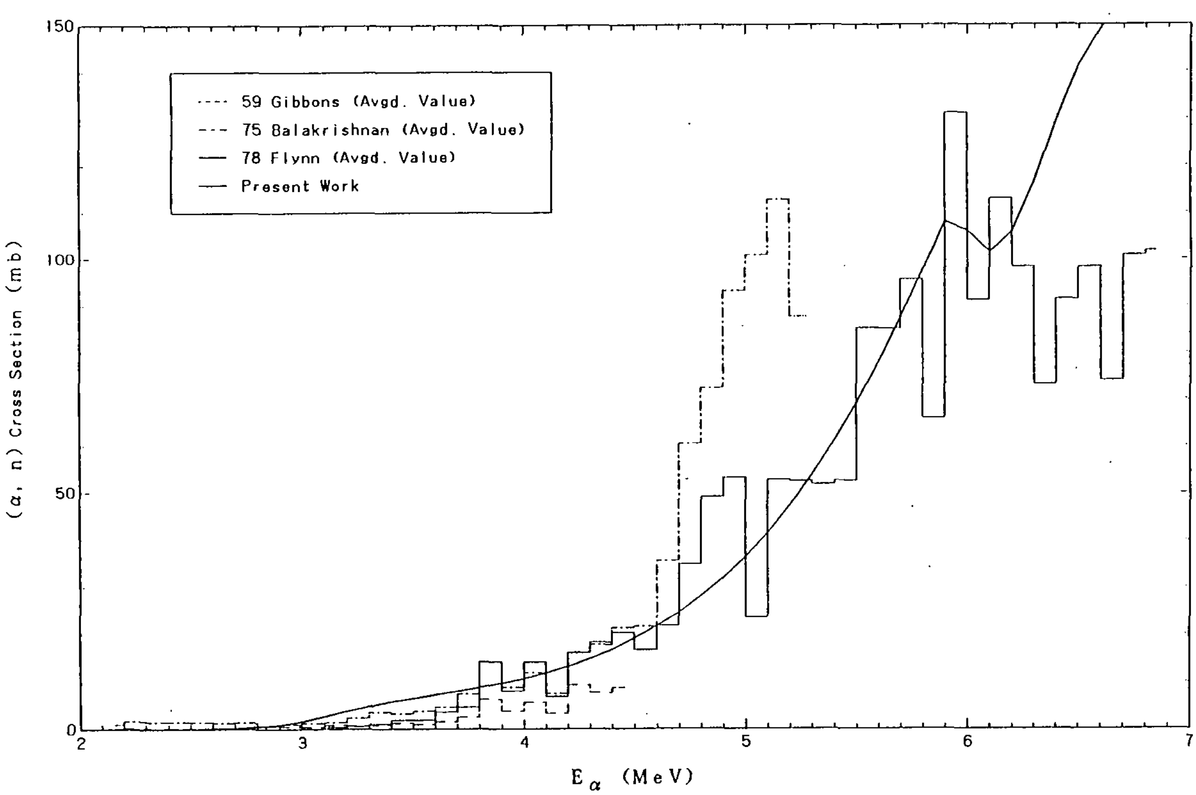

Fig. 4 Comparison of present work and the experimental averaged cross sections for ^{29}Si (α, n) ^{32}S reaction

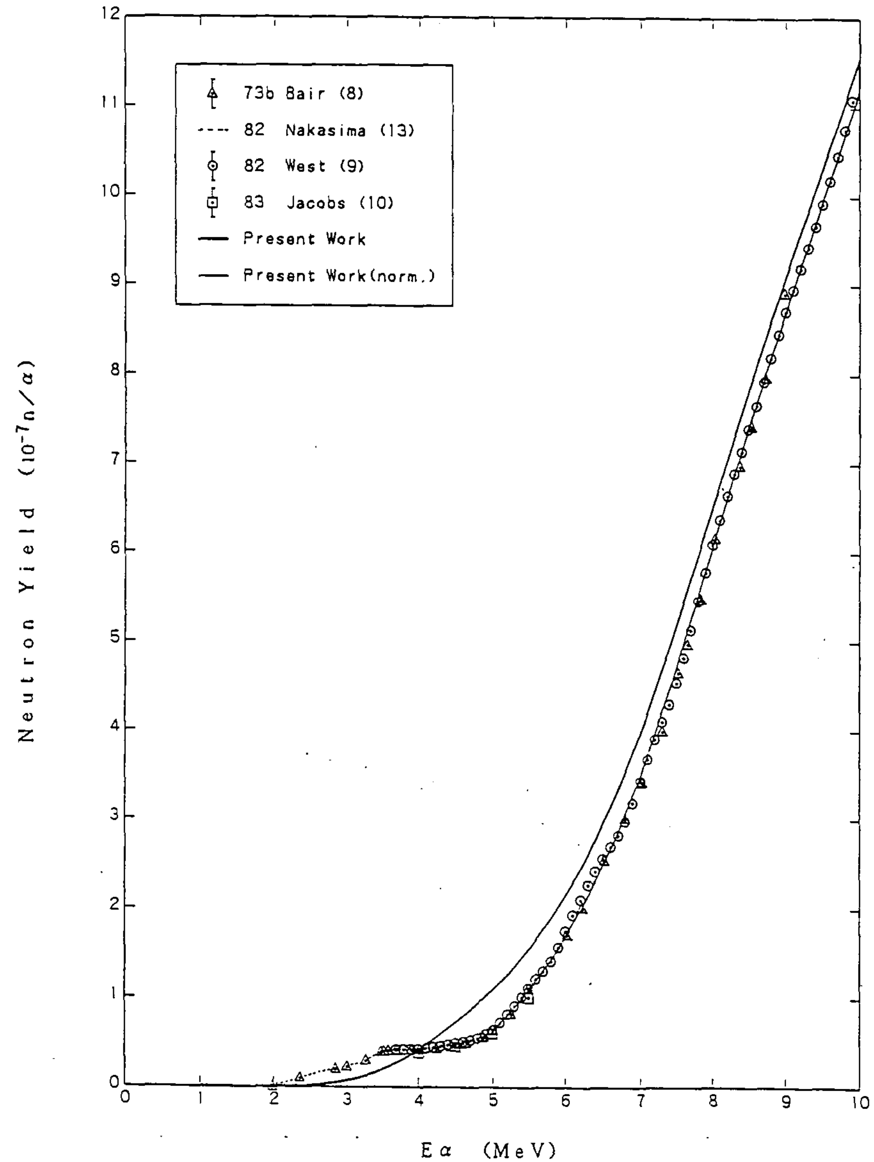

Fig. 5 Neutron Yields in Carbon

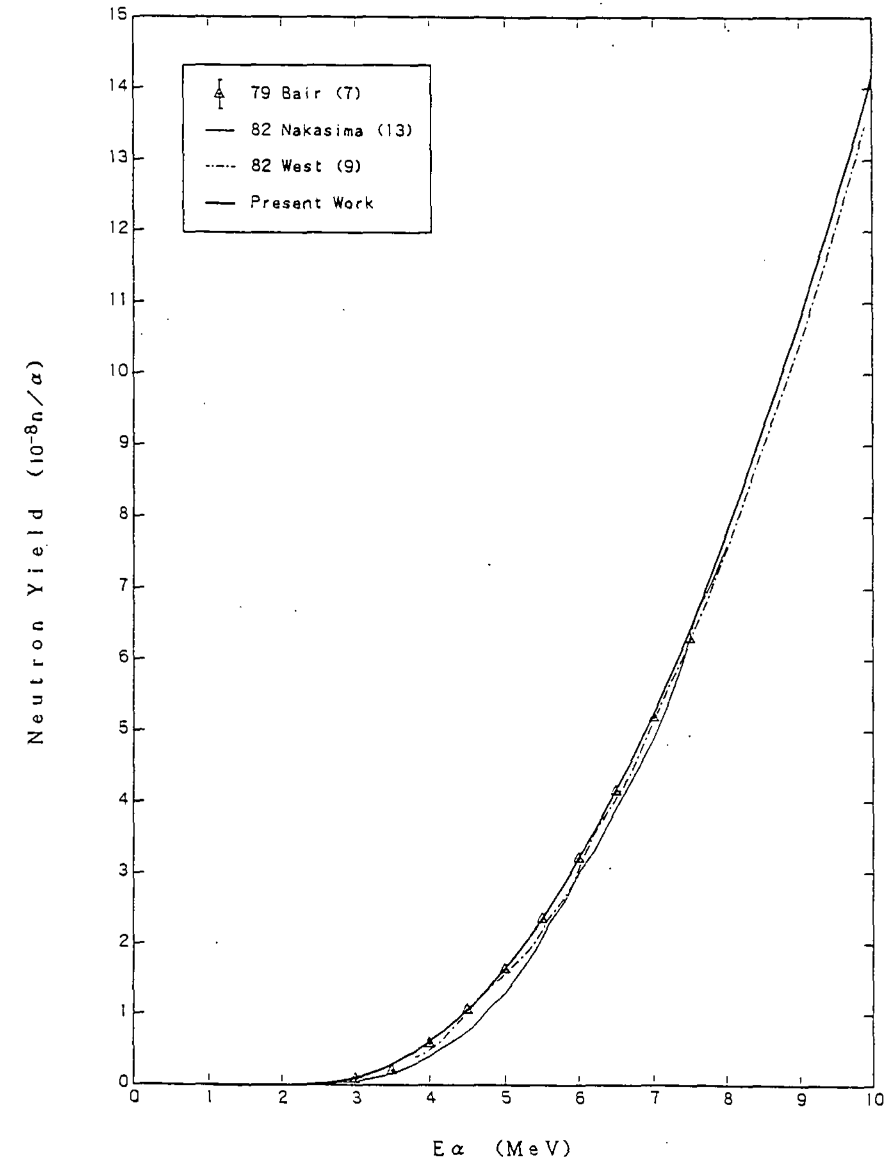

Fig. 6 Neutron Yields in Uranium Oxide

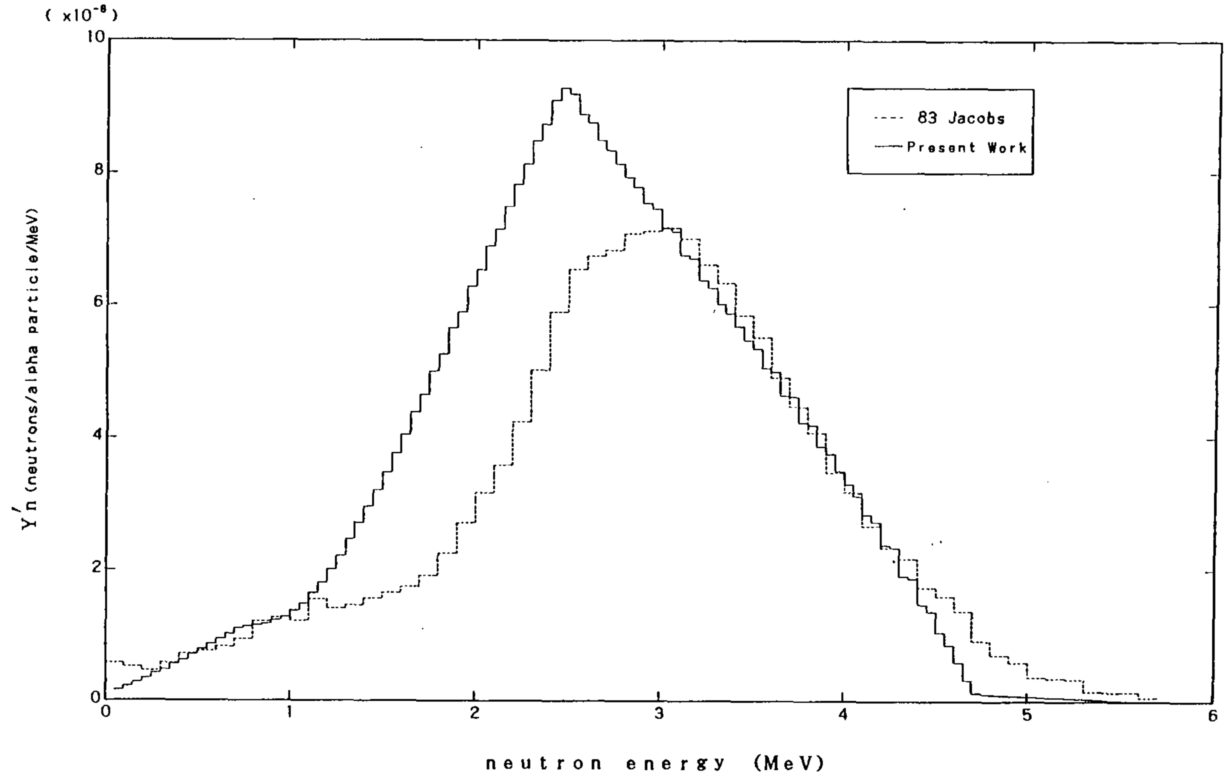

FIG. 7 Neutron Energy Spectrum for Natural Boron at Indicent Alpha Particle Energy=5.0 MeV

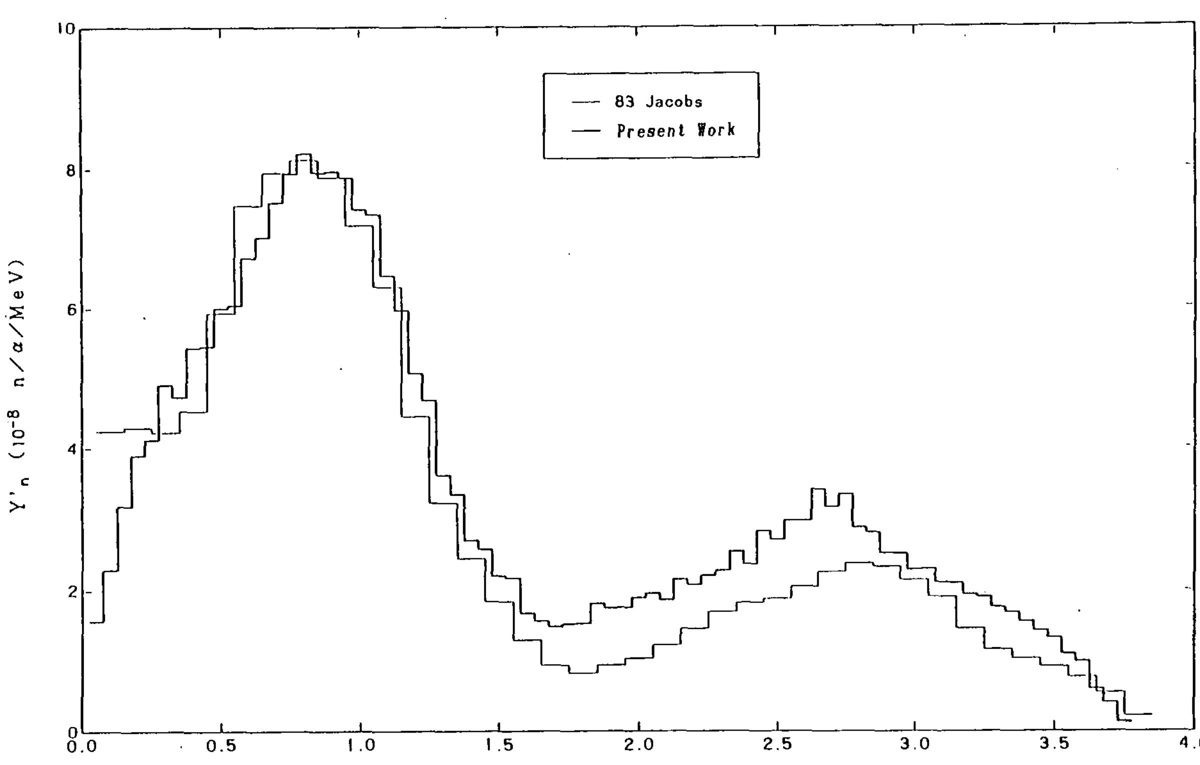

Fig. 8 Neutron energy spectrum from ^{nat}Si (α, n) reaction at incident alpha particle energy = 5.5 MeV

III. Kinki University

A. Atomic Energy Research Institute

III-A-1 Nuclear Data Evaluation for U-232 in the Fast Neutron Region

Takaaki Ohsawa and Toshikazu Shibata

A paper on this subject was published in Annual Reports of Kinki University Atomic Energy Research Institute, Vol. 25, pp.1-12 (December 1988) with the following abstract:

Neutron nuclear data for U-232 were evaluated in the fast neutron region. Because of the insufficiency of the experimental data, evaluation was mostly carried out relying on theoretical models or on semiempirical systematics. The optical model combined with the Hauser-Feshbach-Moldauer formalism was used to calculate the capture and inelastic scattering cross sections. The fission cross section in the MeV region was calculated using the fission probability data obtained from direct-reaction induced fission. The prompt and delayed neutron multiplicities were estimated acccording to the systematics of Bois-Frehaut and Tuttle, respectively. The results of the present evaluation was incorporated into Japanese Evaluated Nuclear Data Library, version 3 (JENDL-3).

III-A-2 <u>Theoretical Methods for the Calculation of Fast Neutron Fission Cross Sections</u>

Takaaki Ohsawa

A paper on this subject was published in the Proceedings of an Advisory Group Meeting on Nuclear Theory for Fast Neutron Nuclear Data Evaluation, IAEA-TECDOC-483 ,IAEA (November 1988), pp.134-147, with the following abstract:

Methods of fission cross section calculation are reviewed and discussed. There are two methods.

The first is utilization of systematics and empirical data. This itself comprises two methods. One is application of systematics observed in fission cross section values in the MeV-region. Another is the use of fission probability data obtained from direct reactions such as (d,pf), (t,pf) in order to produce simulated neutron-induced fission cross sections.

The second method is theoretical model calculation based on the double-humped barrier concept of fission. In this report, the results of our analysis of fission cross sections for 24 actinide nuclides ranging from protactinium to californium are discussed. An attempt has been made to deduce the surface energy coefficient of liquid-drop model from the fision barrier heights obtained in the present analysis.

III-A-3

On the Fission Neutron Spectrum for U-235 in JENDL-3T

Takaaki Ohsawa

A paper on this subject was published in the Proceedings of the 1988 Seminar on Nuclear Data, JAERI-M 89-026 (March 1989) pp.114-120, with the following abstract:

The fission neutron spectrum for U-235 contained in JENDL-3T was compared with those in JENDL-2 and ENDF/B-V. Verification of the spectrum was attempted by comparing the calculated and measured fission-spectrum averaged cross sections for 18 dosimetry reactions.

B. Department of Reactor Engineering

III-B-1

U-235 Fission Neutron Spectrum Averaged Cross Sections Measured for Some Threshold Reactions on Mg, Al, Ca, Sc, Ti, Fe, Co, Ni, Zn, Sr, Mo, Rh, In and Ce

O.Horibe, Y.Mizumoto, T.Kusakabe and H.Chatani*

A paper on this subject has been submitted to the International Conference on the 50 Years with Nuclear Fission, with the following abstract:

The thirty-four averaged cross sections of the (n,p), (n,α), (n,n') and (n,2n) reactions are measured by the activation method relative to that of $^{27}Al(n,\alpha)^{24}Na$ reaction. The samples were irradiated by fission neutrons generated with a U-235 fission plate. The following various kinds of corrections were done for the photo peak areas measured without causing random coincidence; (1) cascade coincidence summing effect due to cascade gammas, (2) contribution of gammas from impurities in the samples and (3) the photo peak efficiencies of a detector due to sizes of the samples. The 34 reaction rate ratios are best estimated from the 113 measured ratios considering correlations between the experimental data. The cross sections obtained assuming the reference one to be 0.705 mb and their correlation matrix are given.

---

* Research Reactor Institute, Kyoto University

IV. Kyoto University

IV-A-1

Gamma-rays and half-life of ^{156}Nd

K. Okano and Y. Kawase

Following the decay of the heaviest isotope of neodymium, ^{156}Nd, only two γ-ray lines of 84.8 and 150.7 keV have hitherto been reported.[1] By using the KUR-ISOL which can produce rather intense NdO ions with high efficiency [2] and a time resolved spectroscopy system equipped with a Canberra X-γ detector, several new γ-ray lines have been identified together with X-rays of Pm. The energy and efficiency calibrations of the X-γ detector were performed by using a set of calibrated γ-ray sources. The detector was heavily shielded for γ-rays as well as for neutrons. As the energy resolution of the large volume X-γ detector for X-rays was only about 0.6 keV, special procedure was necessary to separate the Pm X-rays from those of Sm and this was done by using a spectrum analysis code PDET running on a microcomputer.[3] This code allows rather accurate peak area calculation for complicated spectrum by displaying peak and region parameters as well as the fitted results on-line. For the present X-ray analysis, one of the routines which allows rather complicated peak-shape calibration and calculated-peak-position input mode was employed.

The energies and intensities obtained are listed in Table 1 together with the half-life of each line. The half-life of ^{156}Nd has been determined as 5.51 $\pm$ 0.10 s from the average of half-lives of Pm K_α (5.5 $\pm$ 0.1 s) , Pm K_β (5.5 $\pm$ 0.1 s) and ^{156}Nd γ-rays (5.6 $\pm$ 0.17 s). This is in good agreement with the reported value of 5.47 $\pm$ 0.11 s.[1]

References:

1) R. C. Greenwood, R. A. Anderl and J. D. Cole, Phys. Rev. C 35 (1987) 1965.

2) Y. Kawase and K. Okano, Nucl. Instr. and Meth. B37-38 (1989) 116.

3) K. Okano et al., to be published.

Table 1. Energies, relative intensities and half-lives of X- and γ-rays following the decay of ^{156}Nd.

Ref.1)		Present results		
E_γ (keV)	$T_{1/2}$(s)	E_γ (keV)	$I_{\gamma(X)}$	$T_{1/2}$(s)
Pm K	5.5	Pm K_α	1100(160)	5.5(0.1)
		Pm K_β	270 (40)	5.5(0.1)
		59.8(0.2)	15 (4)	5.7(2.0)
84.8	5.3	84.6(0.1)	63 (11)	6.7(0.9)
150.7	5.3	150.4(0.1)	100	5.4(0.2)
		157.3(0.1)	78 (16)	5.6(1.7)
		161.0(0.3)	35 (5)	6.4(0.7)
		196.7(0.2)	28 (6)	5.9(2.0)
		274.0(0.3)	36 (8)	6.1(0.6)
		319.3(0.3)	32 (5)	5.7(0.6)

IV-A-2 Gamma-rays following the Decays of ^{147}Ba and ^{147}La

K. Aoki†, Y. Kawase and K. Okano

Two studies have been reported on the level structure of ^{147}La through the decay of 0.8 s ^{147}Ba.[1,2] There remain, however, large discrepancies concerning the level and decay scheme in ^{147}La especially as to the existence of the 15.6 keV first excited state. As to the level scheme of ^{147}Ce, three studies have hitherto been reported through the decay of 4.5 s ^{147}La.[1-3] But the excitation energies of levels reported were limited below 1 MeV and the number of lines reported was only about 30~50 in spite of the β-decay Q-value of 4.75 MeV. We have studied the γ-rays and conversion electrons following the decays of these two nuclides using the on-line isotope separator KUR-ISOL.

Singles and coincidence spectra of γ-rays were measured using 142 cc Ge(Li), 132 cc HPGe (X-γ type) and low energy photon spectrometer(LEPS) type detectors. Several kinds of time sequences for beam collection, cooling and time-resolved measurements were employed to enhance the γ-rays associated with the nuclide of interest and to discriminate against those associated with longer-lived isobars. The energy and efficiency calibrations of the detectors were carried out using a set of calibrated γ-ray sources. The spectra were analyzed by a peak analysis program PDET which assures accurate analysis of a complicated spectrum by on-line graphic display of parameters and fitted results utilyzing a microcomputer. The γ-ray energies and relative intensities measured are listed in Tables 1 and 2 for ^{147}Ba and ^{147}La, respectively.

As listed in Table 1, 145 γ-ray lines have been assigned to originate from the decay of 0.8 s ^{147}Ba. These include a lot of unreported lines. A new level scheme consisting of 48 levels has been constructed on the bases of γ-γ coincidence measurements.[4] The existence of the 15.6 keV first excited state

† Himeji Institute of Technology

in ^{147}La was confirmed and 11 new levels have been incorporated. Of measured 145 lines, 143 lines have been fitted into this level scheme.

In the case of the decay of ^{147}La, 93 lines have been assigned altogether with the energies up to 2 MeV. About half of these lines are newly found ones. A new level scheme consisting of 36 levels with excitation energies up to 2.36 MeV has been constructed on the bases of γ-γ coincidence measurements.[4] Of these levels, 7 levels are newly assigned ones. The decay scheme determined incorporated all 93 lines listed in Table 2 and its fundamental structure is not far from that recently reported by Robertson et al.[3]

The results of the conversion electron measurements on the decays of ^{147}Ba and ^{147}La have previously been reported.[5] Further studies on absolute γ-ray yields and γ-γ angular correlations are now in progress.

References:

1) M. Shmid, Y. Y. Chu, G. M. Gowdy, R. L. Gill, H. I. Liou, M. L. Stelts, R. E. Chrien, R. F. Petry, H. Dejbakhsh, C. Chung and D. S. Brenner, Proc. 4th Int. Conf. on Nuclei Far From Stability, ed. by P. G. Hansen and O. B. Nielsen (Skolen, Helsingor, 1981), p.576.

2) F. Schussler, B. Pfeiffer, H. Lawin, E. Monnand, J. Münzel, J. A. Pinston and K. Sistemisch, ibid., p.589.

3) J. D. Robertson, W. B. Walters, S. H. Faller, C. A. Stone, E. M. Baum, P. F. Mantica, R. L. Gill and A. Piotrowski, 5th Int. Conf. on Nuclei Far From Stability, ed. by I. S. Towner(Rosseau Lake, Ontario, Canada, 1987) p.459.

4) K. Aoki, K. Okano and Y. Kawase, Kyoto University Research Reactor Institute Technical Report KURRI-TR-318 (1989) p.83.

5) K. Aoki, T. Mitamura, K. Hiromura, T. Sekioka, Y. Kawase and K. Okano, Research Report of Himeji Institute of Technology, 40A (1987) 1.

Table 1. Energies and intensities of the gamma-rays in the decay of 147Ba

Energy (keV)	Relative Intensity	Energy (keV)	Relative Intensity
15.62 (0.06)	42 (7)	308.37 (0.15)	17 (4)
46.35 (0.12)	30 (3)	308.08 (0.22)	96 (6)
46.33 (0.12)	80 (6)	309.59 (0.06)	107 (10)
61.62 (0.10)	25 (4)	317.17 (0.14)	33 (4)
74.27 (0.08)	404 (15)	318.93 (0.06)	46 (5)
91.11 (0.09)	34 (3)	323.39 (0.06)	38 (6)
92.98 (0.10)	114 (9)	336.6 (0.5)	5 (5)
97.46 (0.12)	79 (6)	338.2 (0.6)	14 (8)
97.55 (0.16)	26 (3)	340.85 (0.10)	23 (8)
105.15 (0.09)	527 (12)	356.16 (0.06)	180 (9)
111.19 (0.09)	10 (3)	355.5 (0.4)	44 (6)
115.06 (0.08)	56 (6)	362.58 (0.06)	132 (8)
120.83 (0.08)	70 (5)	364.47 (0.08)	108 (5)
130.35 (0.11)	25 (3)	365.40 (0.14)	272 (29)
130.65 (0.10)	29 (3)	370.21 (0.06)	34 (5)
140.46 (0.10)	38 (3)	372.61 (0.07)	47 (6)
144.17 (0.06)	67 (6)	374.47 (0.07)	95 (14)
150.08 (0.06)	119 (6)	379.99 (0.07)	51 (8)
157.71 (0.07)	118 (8)	388.0 (0.4)	4 (2)
159.08 (0.09)	180 (8)	395.72 (0.06)	17 (3)
167.45 (0.08)	1000 (20)	399.57 (0.09)	53 (4)
167.83 (0.14)	206 (10)	410.36 (0.14)	17 (6)
175.29 (0.07)	84 (7)	418.4 (0.4)	11 (5)
190.70 (0.06)	70 (12)	421.2 (0.9)	8 (2)
192.9 (0.6)	34 (6)	438.34 (0.07)	21 (5)
196.28 (0.05)	551 (13)	452.49 (0.10)	21 (11)
202.7 (0.4)	8 (4)	455.91 (0.20)	11 (3)
208.7 (0.5)	9 (4)	458.26 (0.07)	24 (6)
211.87 (0.06)	128 (6)	467.62 (0.07)	38 (5)
211.90 (0.06)	28 (6)	473.91 (0.06)	148 (8)
226.45 (0.07)	29 (5)	476.8 (0.6)	73 (11)
233.15 (0.06)	79 (8)	491.5 (0.6)	41 (8)
236.76 (0.06)	63 (5)	502.5 (0.9)	5 (4)
240.6 (0.9)	4 (1)	529.70 (0.29)	11 (3)
241.83 (0.08)	14 (4)	536.18 (0.10)	30 (4)
249.39 (0.06)	396 (15)	541.85 (0.06)	98 (13)
258.94 (0.14)	145 (12)	545.69 (0.08)	48 (10)
260.1 (0.9)	7 (2)	548.8 (0.4)	6 (7)
262.07 (0.08)	95 (5)	558.0 (0.6)	44 (6)
262.81 (0.08)	36 (4)	566.13 (0.08)	22 (12)
264.94 (0.06)	90 (5)	591.53 (0.10)	35 (5)
268.63 (0.11)	44 (4)	598.14 (0.09)	78 (11)
277.0 (0.6)	16 (4)	602.83 (0.30)	52 (9)
278.36 (0.07)	41 (6)	613.86 (0.10)	18 (5)
292.24 (0.12)	71 (8)	622.56 (0.13)	25 (15)
294.59 (0.06)	29 (3)	644.45 (0.07)	27 (5)
297.92 (0.10)	22 (4)	657.29 (0.06)	19 (5)
298.23 (0.10)	27 (4)	659.9 (0.6)	26 (6)
304.89 (0.06)	63 (6)	689.07 (0.08)	47 (14)

Energy (keV)	Relative Intensity
735.00 (0.28)	24 (21)
743.63 (0.07)	62 (17)
798.6 (0.4)	25 (9)
811.12 (0.08)	28 (12)
838.31 (0.15)	14 (9)
885.32 (0.09)	49 (15)
894.46 (0.21)	100 (26)
925.10 (0.12)	75 (16)
937.35 (0.11)	20 (5)
949.80 (0.06)	32 (11)
977.72 (0.15)	58 (23)
1022.62 (0.09)	22 (10)
1038.92 (0.11)	74 (22)
1054.67 (0.10)	47 (6)
1056.06 (0.09)	104 (19)
1059.20 (0.10)	42 (9)
1092.38 (0.07)	14 (4)
1107.41 (0.10)	62 (12)
1115.07 (0.16)	25 (9)
1151.37 (0.15)	33 (8)
1170.72 (0.13)	14 (5)
1173.04 (0.34)	20 (11)
1174.08 (0.21)	19 (11)
1240.17 (0.27)	37 (7)
1249.01 (0.12)	36 (14)
1268.23 (0.11)	48 (18)
1268.39 (0.09)	22 (16)
1283.6 (0.6)	16 (6)
1355.14 (0.08)	41 (26)
1361.70 (0.27)	34 (10)
1365.60 (0.10)	72 (26)
1385.25 (0.13)	56 (27)
1407.94 (0.06)	47 (15)
1431.47 (0.08)	68 (27)
1436.26 (0.15)	19 (8)
1450.09 (0.09)	56 (17)
1468.04 (0.09)	40 (11)
1476.95 (0.15)	24 (11)
1493.0 (0.6)	11 (6)
1517.48 (0.06)	297 (27)
1524.75 (0.09)	16 (6)
1530.33 (0.11)	29 (37)
1533.41 (0.27)	41 (23)
1588.85 (0.09)	30 (10)
1636.83 (0.15)	38 (21)
1683.78 (0.11)	51 (22)
1757.81 (0.10)	165 (19)

Table 2. Energies and intensities of the gamma-rays in the decay of 147La

Energy (keV)	Relative Intensity	Energy (keV)	Relative Intensity
69.01 (0.11)	48 (3)	421.71 (0.15)	21 (6)
100.28 (0.13)	21 (3)	426.46 (0.08)	20 (7)
103.66 (0.10)	34 (4)	430.43 (0.08)	25 (9)
117.56 (0.08)	1000 (18)	432.87 (0.07)	95 (7)
138.45 (0.41)	7 (2)	437.1 (0.6)	31 (5)
141.13 (0.26)	43 (5)	438.30 (0.06)	400 (25)
152.06 (0.13)	26 (4)	438.47 (0.12)	48 (16)
156.39 (0.09)	66 (4)	440.29 (0.09)	37 (5)
156.38 (0.09)	17 (4)	462.08 (0.28)	22 (7)
164.3 (0.6)	22 (5)	468.9 (0.6)	16 (3)
170.37 (0.07)	25 (5)	477.88 (0.26)	29 (6)
172.68 (0.11)	30 (2)	480.1 (0.6)	17 (5)
184.67 (0.10)	19 (3)	490.84 (0.07)	28 (6)
186.50 (0.11)	99 (6)	490.93 (0.11)	23 (6)
186.89 (0.11)	530 (19)	495.32 (0.06)	112 (8)
207.55 (0.07)	24 (9)	505.92 (0.09)	33 (7)
215.06 (0.05)	208 (10)	507.85 (0.10)	106 (11)
215.27 (0.15)	489 (13)	517.21 (0.08)	241 (20)
218.15 (0.07)	66 (10)	520.33 (0.14)	20 (7)
225.28 (0.07)	29 (5)	523.69 (0.07)	35 (21)
235.69 (0.06)	234 (10)	557.75 (0.09)	42 (9)
239.2 (0.4)	5 (3)	557.75 (0.09)	34 (6)
246.35 (0.06)	47 (4)	570.89 (0.06)	38 (4)
272.61 (0.08)	46 (10)	570.95 (0.08)	59 (6)
273.88 (0.10)	163 (6)	586.19 (0.08)	22 (4)
279.97 (0.06)	55 (7)	591.79 (0.12)	51 (6)
283.47 (0.07)	231 (19)	599.25 (0.09)	65 (7)
289.97 (0.14)	33 (10)	602.28 (0.11)	26 (7)
292.61 (0.10)	20 (15)	645.0 (0.6)	54 (7)
308.11 (0.08)	46 (7)	647.18 (0.15)	31 (8)
318.65 (0.14)	35 (5)	652.08 (0.12)	11 (6)
320.71 (0.06)	39 (5)	668.94 (0.25)	24 (6)
332.75 (0.08)	67 (8)	673.84 (0.08)	17 (7)
334.37 (0.11)	15 (5)	710.27 (0.18)	52 (10)
334.55 (0.17)	13 (5)	767.2 (0.4)	3 (2)
342.77 (0.10)	13 (3)	773.13 (0.16)	14 (4)
353.33 (0.06)	161 (15)	786.0 (0.4)	8 (4)
377.38 (0.07)	54 (6)	854.2 (0.6)	17 (5)
382.42 (0.29)	12 (4)	900.5 (0.6)	16 (5)
387.77 (0.14)	62 (6)	974.80 (0.08)	16 (6)
390.84 (0.06)	15 (4)	1548.24 (0.22)	31 (10)
393.50 (0.10)	33 (7)	1784.06 (0.06)	29 (14)
399.58 (0.09)	146 (5)	1953.6 (0.6)	15 (8)
399.66 (0.13)	63 (3)	2000.6 (0.6)	30 (10)
401.77 (0.08)	133 (14)	2022.5 (0.6)	16 (8)
410.66 (0.09)	33 (7)	2026.6 (0.6)	19 (8)
416.82 (0.14)	18 (4)		

IV-A-3

Neutron Total Cross Section Measurements of Sb

K. Kobayashi, S. Yamamoto, S. M. Lee*, Y. Fujita,
I. Kimura** and S. Kanazawa**

By making use of the 46 MeV electron linear accelerator at the Research Reactor Institute, Kyoto University (KURRI), transmission measurements have been made on six sample thicknesses of natural antimony, Sb. The purity of the sample was 99.9 % and the powder sample was packed in a cylindrical acryl case with Al windows. The data from 0.01 eV to several eV and from a few keV to a few MeV were obtained using a ^{6}Li glass scintillation detector at 22.2 m flight path. The experimental method and data reduction is same as before[1]. The present results are shown in Figs. 1 and 2, where the TOF data were summed in every 0.1 lethargy unit. In the lower energy region (Fig. 1), Mughabghab's evaluation[2] seems to be higher. For the hundreds of keV range (Fig. 2), there is a large deviation among the previous data. The eye-guide curve by Mughabghab is close to the present measurement.

Moreover, we have applied a resonance capture detector[3] to the measurement of the neutron total cross section of Sb. Indium and gold samples were used for the neutron transmission measurements at the resonances of 1.46 eV for In and 4.91 eV for Au, respectively. The results at these energy points support the above energy dependent data measured presently with white neutrons, as seen in Fig. 3.

---

* Indira Gandhi Centre for Atomic Research, Kalpakkam 603-102 India.

** Dept. of Nucl. Eng., Faculty of Eng., Kyoto University Yoshida-honmachi, Sakyo-ku, Kyoto 606 Japan

References:

1) K. Kobayashi, et al.:Ann. Nucl. Energy, Vol.15, 381 (1988).

2) V. MacLane, et al.(Ed.): "Neutron Cross Sections", Vol.2, Neutron Cross Section Curves, Academic Press, Inc. (1988).

3) K. Kobayashi, et al.: JAERI-M 89-026, p.198 (1989).

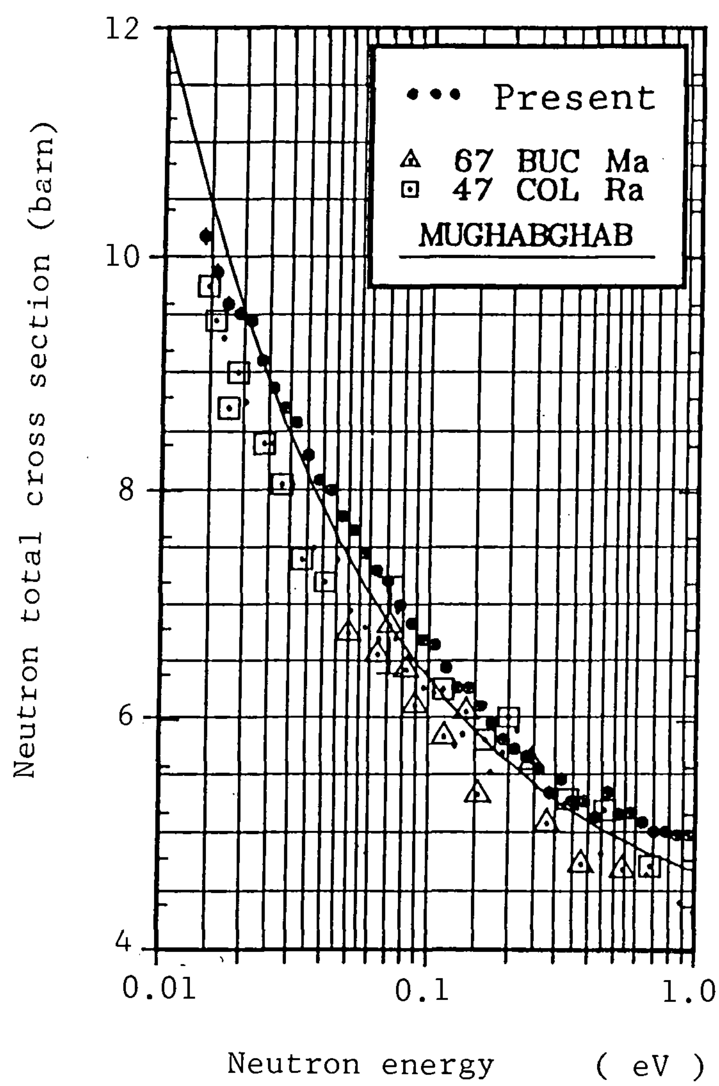

Fig. 1 Neutron total cross section of Sb.

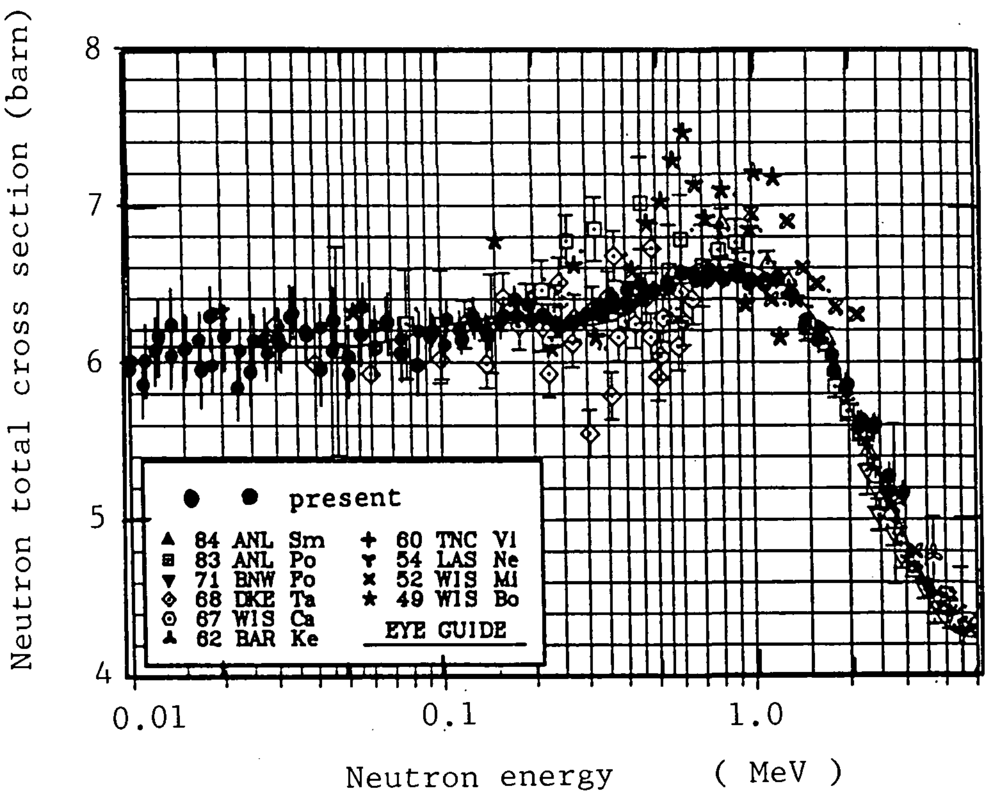

Fig. 2 Neutron total cross section of Sb.

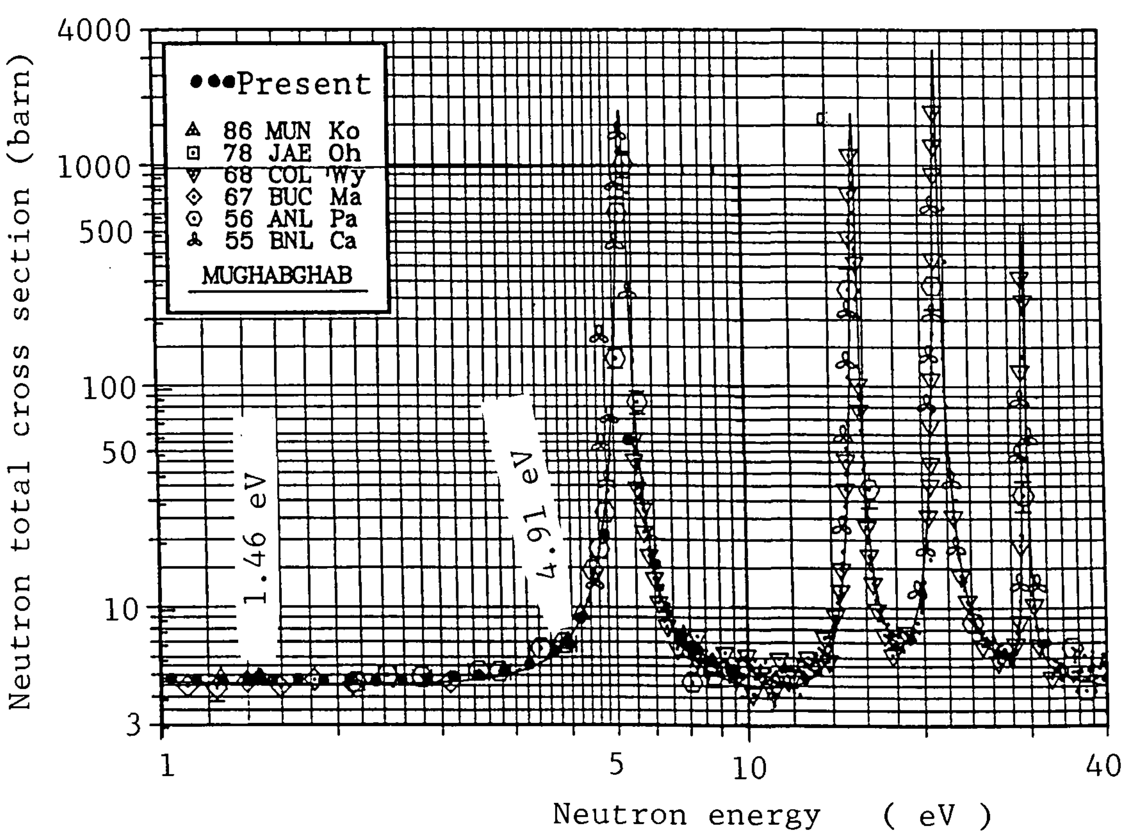

Fig. 3 Neutron total cross section of Sb, comparing with the point data at 1.46 and 4.91 eV.

IV-A-4 Experimental Study of Resonance Interference Between Th-232 and U-233

Y. Fujita, K. Kobayashi, S. M. Lee* and I. Kimura**

In advanced thermal and/or fast breeder reactors based on U-233/Th fuel, there are resonance cross section interference effects between the nuclides. Direct measurement of such interference effects is useful for validation of the multigroup cross section processing procedures in which various approximations are made in the treatment of resonance overlap and resonance interference.

An experiment to directly measure the resonance overlap effects between Th-232 and U-233 was carried out by the neutron time-of-flight (TOF) method using the 46 MeV electron linear accelerator (linac) at the Research Reactor Institute, Kyoto University (KURRI). The neutron beam transmitted through a thorium sheet of various thickness (0.5 mm, 1 mm, 1.5 mm, 1/8", 1/4", 1/2", 1" and 3/2") was allowed to traverse a 6.5 m flight path and impinged on a U-233 sample, and the fission (and capture) gammas from the sample were measured, using a pair of C_6D_6 scintillators, in 2048 TOF channels. The same measurement was also performed using a boron sample in place of the U-233 sample. Comparison of the neutron attenuation as a function of thorium thickness for the U-233 and boron samples enables evaluation of the resonance overlap effect in different energy regions.

From the transmission measurements using boron sample, one can calculate the transmission ratio given by,

---

* Indira Gandhi Center for Atomic Research, Kalpakkam 603-102 India.

** Dept. of Nucl. Eng., Faculty of Eng., Kyoto University Yoshida-honmachi, Sakyo-ku, Kyoto 606 Japan.

$$T_g(t) = \frac{\int_{\Delta Eg} e^{-\Sigma_t t} S(E)dE}{\int_{\Delta Eg} S(E)dE}$$

where Σ_t is the total macroscopic cross section of Th. Similarly from the measurements using U-233 sample one can calculate the indication ratio given by,

$$R_g(t) = \frac{\int_{\Delta Eg} \sigma_x^i(E)\, e^{-\Sigma_t t} S(E)dE}{\int_{\Delta Eg} \sigma_x^i(E)\, S(E)dE}$$

where $\sigma_x^i(E)$ is the indication sample of U-233.

From the experimental measurements of $T_g(t)$ and $R_g(t)$, one can evaluate,

$$\int_0^\infty T_g(t)dt = \frac{\int_{\Delta Eg} \frac{1}{\Sigma_t(E)} S(E)dE}{\int_{\Delta Eg} S(E)dE}$$

$$\int_0^\infty R_g(t)dt = \frac{\int_{\Delta Eg} \frac{\sigma_x^i(E)}{\Sigma_t(E)} S(E)dE}{\int_{\Delta Eg} \sigma_x^i(E)\, S(E)dE}$$

Thus, one can obtain the ratio of the self-shielded cross section of reaction x of isotopr i to the infinite dilution cross section for the same reaction.

$$\frac{\int_0^\infty R_g(t)dt}{\int_0^\infty T_g(t)dt} = \frac{\int_{\Delta Eg} \frac{\sigma_{c+f}^{U-233}(E)}{\sigma_t^{Th}(E)} \cdot \frac{dE}{E}}{\int_{\Delta Eg} \frac{1}{\sigma_t^{Th}(E)} \cdot \frac{dE}{E}} \Bigg/ \frac{\int_{\Delta Eg} \sigma_{c+f}^{U-233}(E) \cdot \frac{dE}{E}}{\int_{\Delta Eg} \frac{dE}{E}}$$

In the case the resonance overlap and interference is negligible the ratio will be near unity. The deviation of the ratio from unity indicates the degree of resonance overlap correction in the different energy groups. If there is appreciable overlap effect in some of the energy groups then the measured data provides useful information for testing the capability of the nuclear data files and the processing codes to reproduce this effect.

Figure 1 shows the experimental arrangement for the transmission and indication measurements. Typical time-of-flight spectra are shown for B-10 and U-233 samples in Figs.2 (a) and (b), respectively. The spectra were obtained with a 0.5 mm Cd overlap filter, and the background spectra were determined by the notch filters using Na, Mn, Co and Ag. The high background level for U-233 comes from the gamma rays of the daughter nuclides in the U-decay chain.

Preliminary results of transmission and indication curves vs. the thickness of transmission samples are shown in Figs.3 (a), (b), (c), (d). The case (a) is the energy region bunched between 4 and 30 keV which is the unresolved energy region for both of U-233 and Th. The transmission and indication curves are close each other and the ratio is near unity as a priori expected, since many resonances are involved in the energy interval and the statistical treatment is justified. The cases (b) and (c) are for energy regions, resolved for Th and unresolved for U-233 in the evaluation file, such as JENDL. The ratios deviate from unity in these cases, and the deviation may indicate that one cannot ignore the interference effect in the treatment of cross sections in this energy range. In other words, one need to raise the lower energy limit, 100 eV, of the unresolved energy region of U-233 to a higher value. The case (d) is an example of curves in the energy where dominant resonances of Th and U-233 overlap.

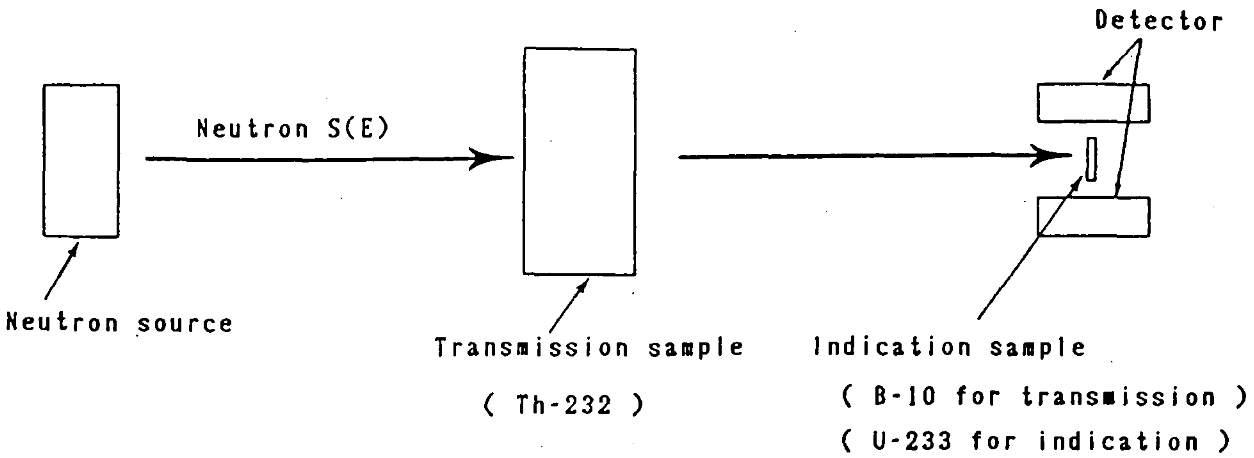

Fig. 1 Arrangement of the transmission and indication experiment.

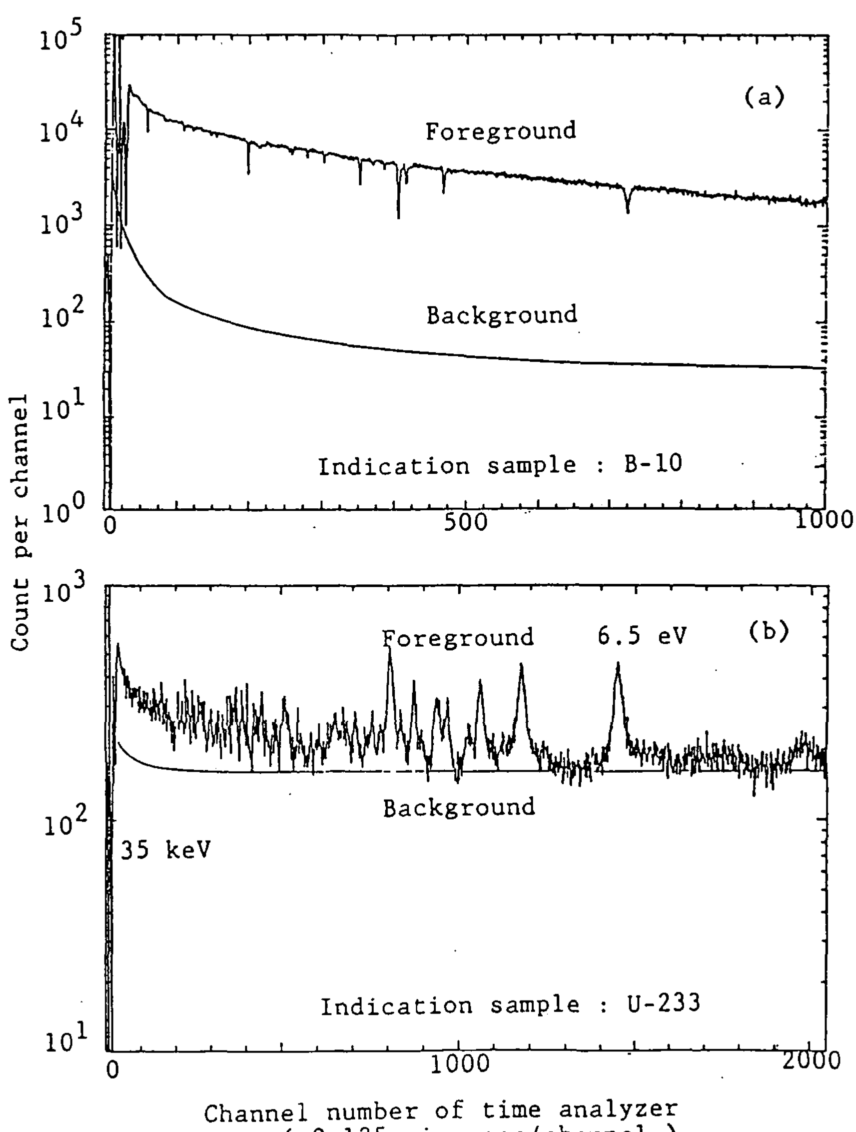

Fig. 2 Typical time of flight spectra of the C_6D_6 detector, (a) for B-10 and (b) for U-233 samples.

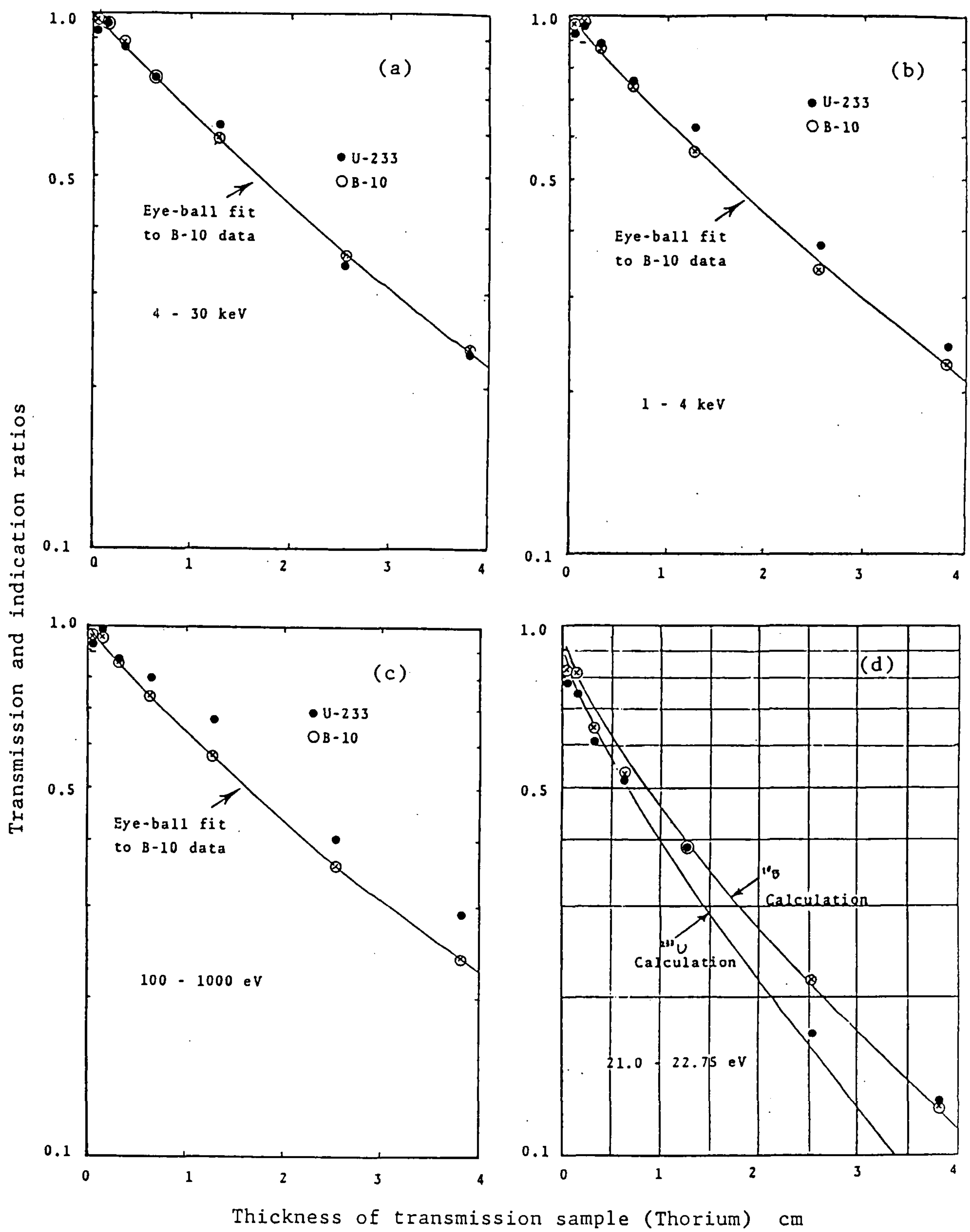

Fig. 3 Transmission and indication ratios vs. thicknesses of transmission sample, (a) for 4-30 keV, (b) for 1-4 keV, (c) for 100-1000 eV and (d) 21.0-22.75 eV.

IV-A-5

The Measurement of Leakage Neutron Spectra from Various Sphere Piles with 14 MeV Neutrons - Ti, As, Se and Zr -

Chihiro Ichihara, Shu A. Hayashi, Katsuhei Kobayashi, Itsuro Kimura*, Junji Yamamoto**, and Akito Takahashi**

In order to check the existing nuclear data files, neutron leakage spectra from various kinds of sphere piles have been measured. Measured samples include Ti, As, Se and Zr. The powdered samples were packed in the spherical shells made of stainless steel, the thickness of which were 2mm or 5mm (Figs.1 and 2). The tritium target was set at the center of the piles. The sample thickness was 0.4 to 2.0 mean free paths for 14 MeV neutrons as shown in the Table-1.

MEASUREMENT

The measurement was done at the intense pulsed neutron source, OKTAVIAN by using the time-of-flight (TOF) method. The neutron detector was NE218 liquid organic scintillator located at 10.75m from the tritium target. To minimize the scattered neutrons, the collimator made of iron-polyethylene multi-layers was set between the pile and the detector (Fig.3).

*Dept. of Nuclear Eng., Kyoto University

**Dept. of Eng., Osaka University

We determined the detector efficiency by combining the Monte Carlo calculation and the TOF measurement of ^{252}Cf and graphite sphere. For the run-to-run monitor, the niobium and aluminum activation foils were irradiated during each measurement.

CALCULATION

The obtained data were compared with the theoretical calculation. MCNP Monte Carlo neutron transport code was used for this purpose. The cross section libraries processed from the evaluated nuclear data files, ENDF/B-IV and ENDL-85 were used for this calculation. As we found no evaluated data file for selenium, the calculation for selenium pile was not done.

RESULTS AND CONCLUSION

The measured and calculated spectra are shown in the Fig. 4. It appears that all three data files have several problems as the followings.

1) Ti : The abrupt change of the calculated spectrum can be observed. This implies that the inelastic continuum scattering cross section and other non-elastic scattering reaction such as (n,2n) reaction are not consistent.

2) As : The shape of the calculated spectrum was quite different from the measured one. It can be considered that possibly (n,2n) cross sections are not correctly evaluated.

3) Zr : The shape of the calculated spectrum between 600 keV and 14 MeV differs considerably. This suggests that inelastic continuum and/or (n,2n) cross sections have to be re-evaluated.

Pile	Dia. (cm)	Sample-Thick. (cm)	(MFPs)	Calc. Code	Data Library
Ti	40	9.8	0.5	MCNP	ENDF/B-IV
As	40	9.8	0.8	MCNP	ENDL-85
Se	40	9.8	0.6	--	--
Zr	60	27.5	2.0	MCNP	ENDL-85

Table 1 The characteristic parameters of the piles, calculation codes and nuclear data files used

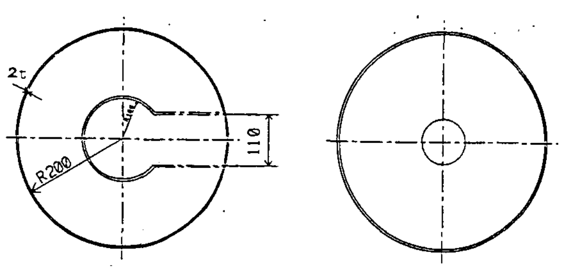

Fig. 1 40 cm pile for use with Ti, As and Se sample

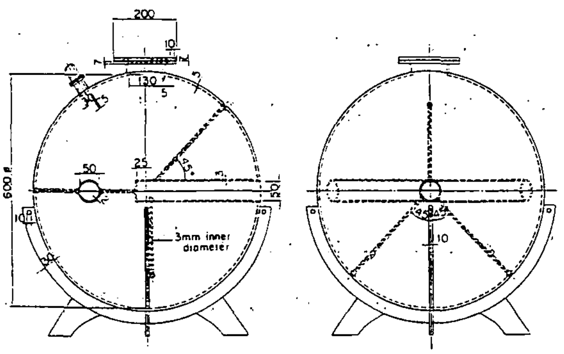

Fig. 2 60 cm pile for use with Zr sample

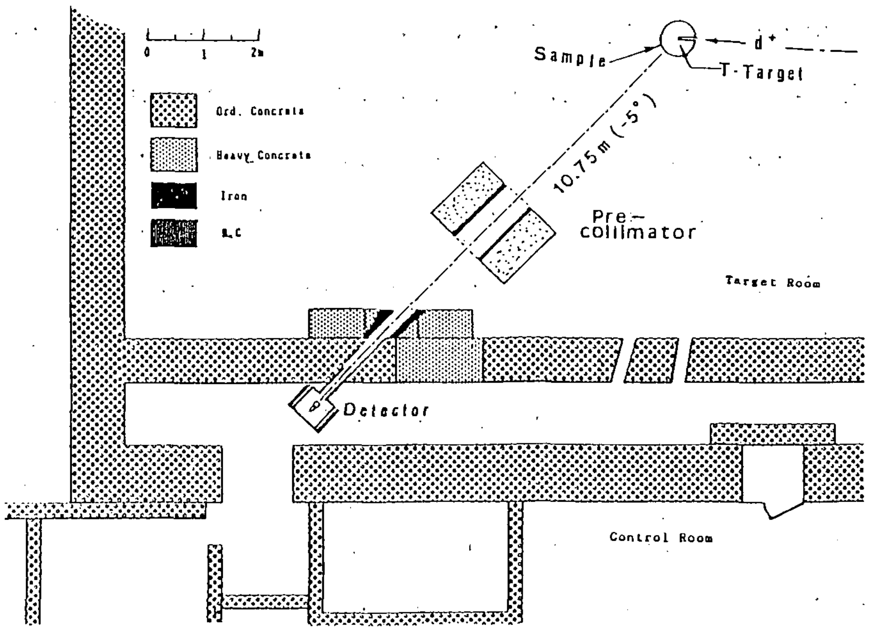

Fig. 3 The experimental arrangement in OKTAVIAN facility

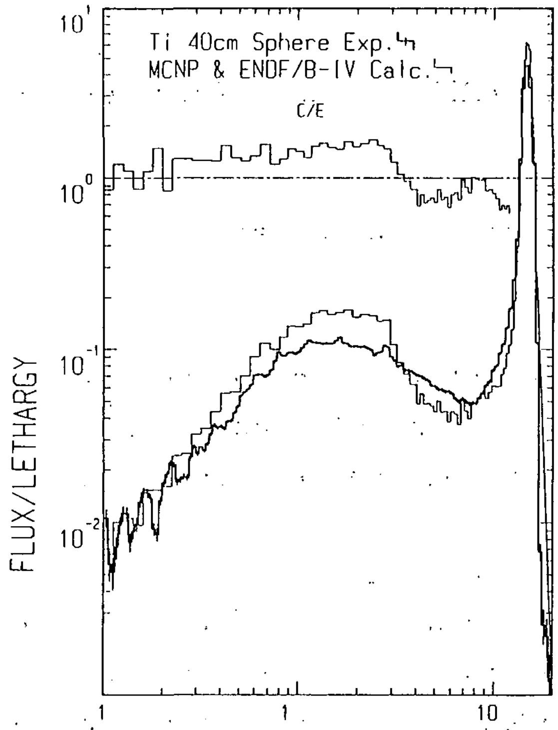

a) Ti 40 cm pile

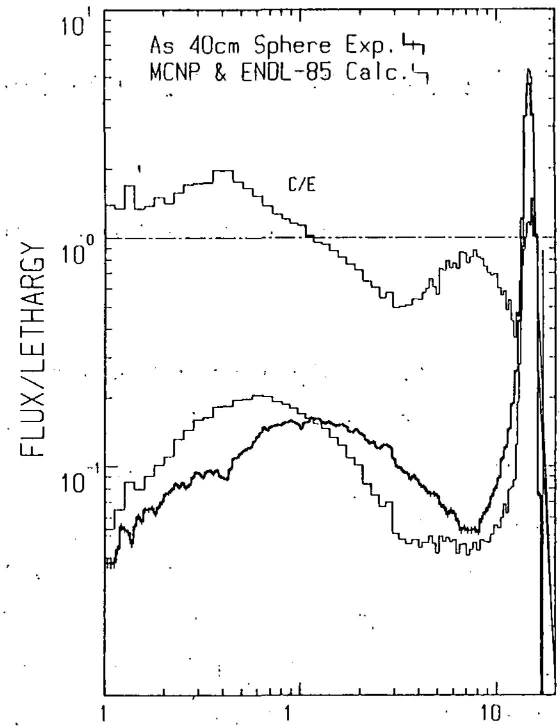

b) As 40 cm pile

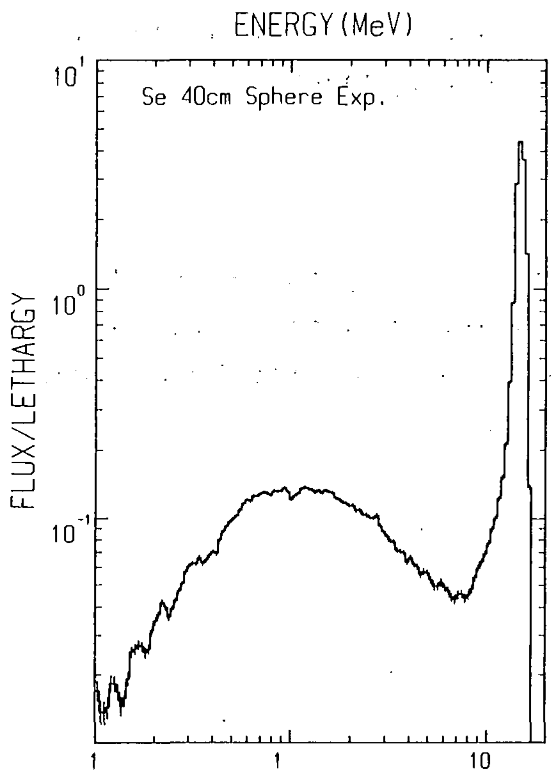

c) Se 40 cm pile

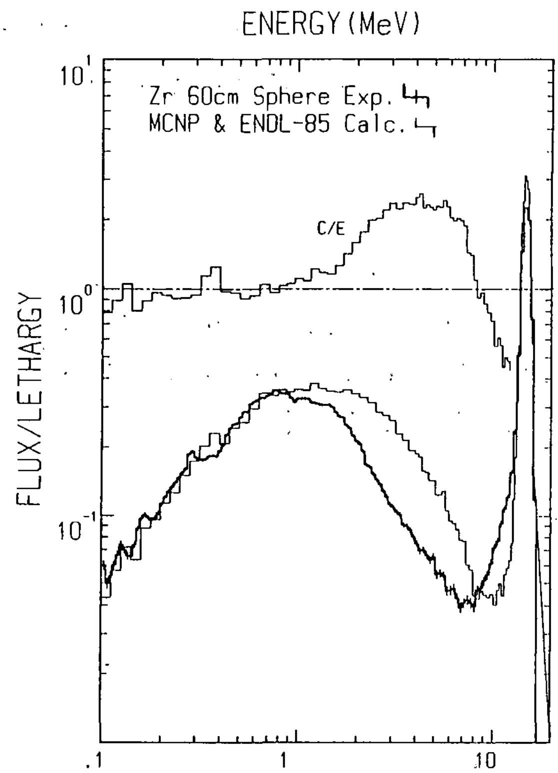

d) Zr 60 cm pile

Fig. 4 The experimental and calculated spectra

IV-A-6

BGO Detectors for Neutron Capture Cross Section Measurements

S. Yamamoto, Y. Fujita and K. Kobayashi

A total absorption gamma-ray detector has been made using 12 BGO scintillator bricks of 5 x 5 x 7.5 cm^3 with an incentive to study the possibility of BGO for neutron capture cross section measurements[1,2].

The detection efficiency has been measured by a neutron time-of-flight spectrometer at the Research Reactor Institute, Kyoto University (KURRI). Sm, Cd, In, Au and Fe samples were employed for capture event measurements, and the efficiency was found between 80 to 100 %.

Very recently, we are applying the BGO detectors to the measurement of absolute capture cross sections of Au and Sb, by using the saturation region at their big resonances.

References:

1) S. Yamamoto, et al.: Nucl. Instr. Meth., A249 484 (1986).
2) S. Yamamoto, et al.: Proc. Int. Conf. on Nucl. Data for Sci. and Technol., held at Mito, Japan (1988), Edited by S. Igarasi, JAERI, p.375 (1988).

IV-A-7

Calibrated Fission and Fusion Neutron Fields

Itsuro Kimura* and Katsuhei Kobayashi

A paper on this subject was submitted to Nuclear Science and Engineering, with the following abstract:

A brief review is given about two thermal neutron driven fast neutron fields, the fission plate and the ^{6}LiD converter. As example of these fields, introduced are the characteristics of a big fission plate (27 cm in diameter and 1.1 cm thick) made of highly enriched uranium and a sandwich type ^{6}LiD converter (2 ^{6}LiD plates 10 x 10 cm square and 1 cm thick), both of which have been used at the heavy water thermal neutron facility of Kyoto University Reactor, KUR. The neutron spectra in the both fields were calculated by MCNP for the former and ANISN for the latter. The average neutron energy and the neutron spectrum of the ^{6}LiD converter were measured and the results agreed with the predicted values. By making use of the both fields, we measured average cross sections for some threshold reactions, 6 with the fission plate and 23 with the ^{6}LiD converter. The results are compared with evaluated values and the previous data.

The experimental arrangement for the big fission plate is illustrated in Fig. 1, and Fig. 2 shows the ratio of the Watt spectrum and the MCNP calculation to the Maxwellian.

---

* Dept. of Nuclear Eng., Faculty of Eng., Kyoto University
Yoshida-honmachi, Sakyo-ku, Kyoto 606 Japan

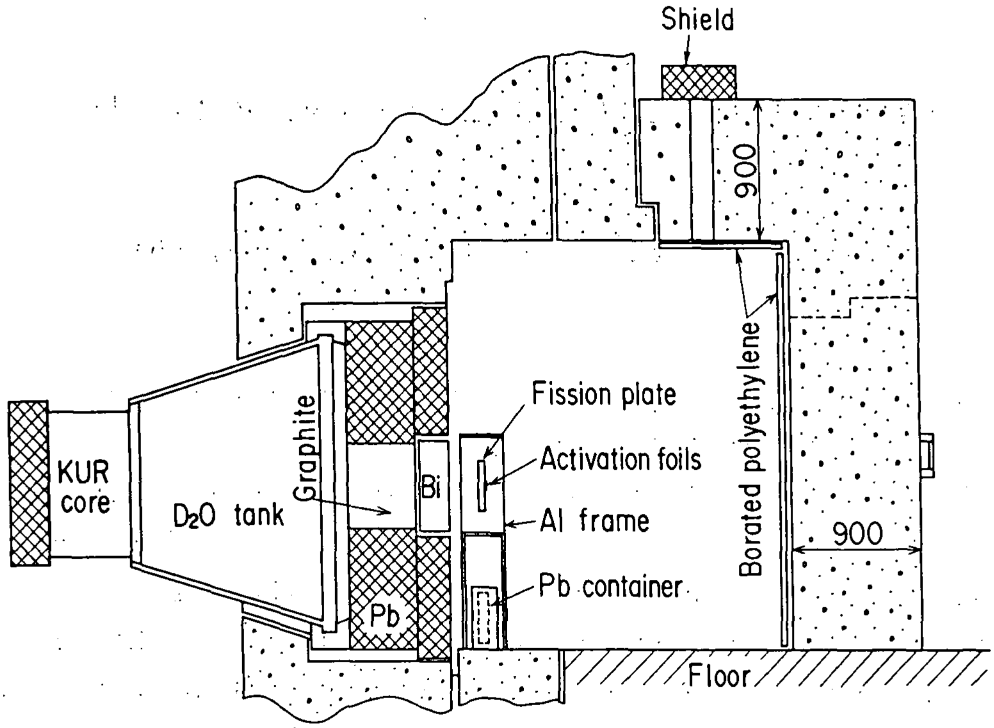

Fig. 1 Experimental arrangement of the big fission plate at the heavy water thermal neutron facility of Kyoto University Reactor, KUR.

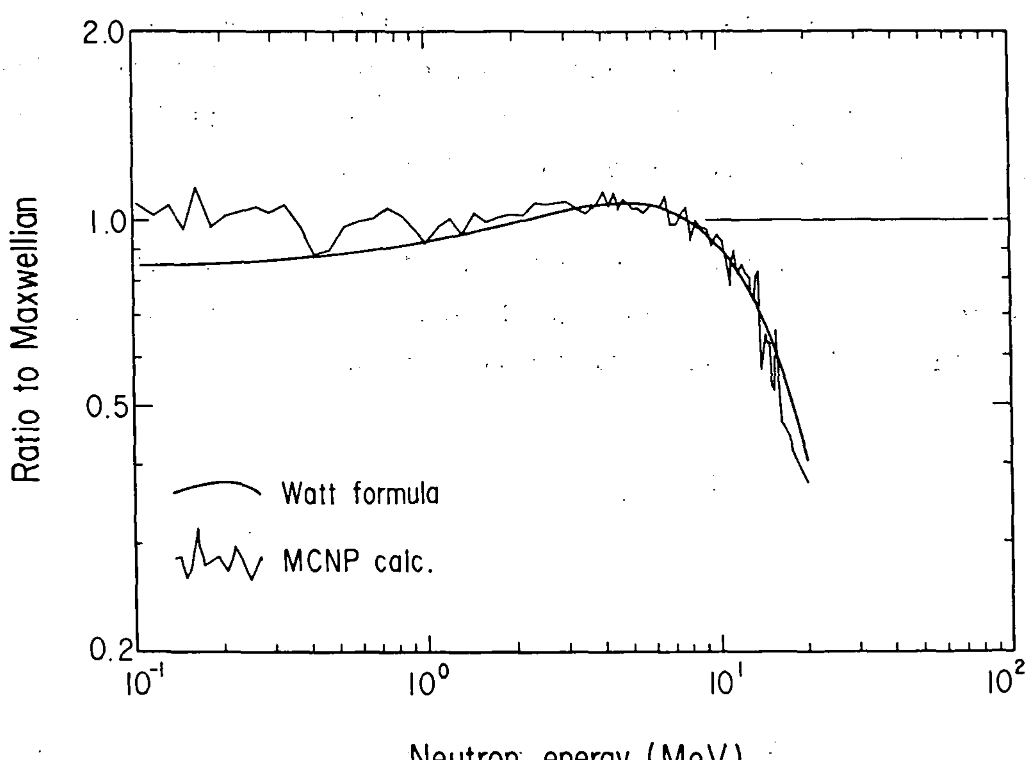

Fig. 2 Comparison of the ratio of the Watt spectrum and the MCNP calculation to the Maxwellian.

V. Kyushu University

A. Department of Nuclear Engineering

Faculty of Engineering

V-A-1

Alpha-particle Energy Spectra from the (p,α) Reaction on Nuclei around Atomic Number 50

I. Kumabe, Y. Inenaga, M. Hyakutake, N. Koori, Y. Watanabe, K. Ogawa, and K. Orito

A paper on this subject was published in Physical Review C 38 (1988) 2531-2540 with the following abstract:

The energy spectra of α particles emitted from (p,α) reactions on ^{112}Cd, ^{118}Sn, ^{120}Sn, Sb, ^{128}Te, and ^{130}Te with 18 MeV protons have been measured in order to clarify the shell and odd-even effects in the preequilibrium processes of (p,α) and (n,α) reactions. From the experimental results, it was found that there exist no appreciable shell and odd-even effects on target nuclei in the gross (p,α) energy spectra lower than 20 MeV in the preequilibrium process. They can be explained well by the knockout model using the effective Q values which are shell independent. The fine structures of the energy spectra for the (p,α) reactions on nuclei around atomic number 50 can be qualitatively explained using the three-nucleon pickup model under the assumption that the states excited in the (p,α) reaction are formed by the coupling of two-neutron-hole states excited in the reaction such as the (p,t) reaction and one-proton-hole states excited in the reaction such as the (d,^{3}He) reactions. The similar three-nucleon pickup model can explain qualitatively the fine structures of the energy spectra for the (n,α) reactions on nuclei around neutron number 50 and 82.

V-A-2

Preequilibrium Model Analysis of (p,n) Reactions on Nuclei in the Cr-Ni Region.

Isao Kumabe and Yukinobu Watanabe

A paper on this subject will be soon published in Physical Review with the following abstract:

The energy spectra of neutrons emitted from 25 MeV (p,n) reactions on nuclei in the Cr-Ni region have been analyzed in terms of the preequilibrium exciton model introducing effective Q values, the pairing correlation, and the modified uniform spacing model in which the uniform spacing model is modified so as to have a wide spacing at the magic number. The calculated energy spectra using the above model are in fairly good agreement with the observed spectra with pronounced structures.

V-A-3

Systematics and Parameterization of Continuum Angular Distributions for Application to Reactions Induced by 14 MeV Neutrons

Isao Kumabe, Yukinobu Watanabe, Yoshimitsu Nohtomi, and Mitsuru Hanada

A paper on this subject will be soon published in Nuclear Science and Engineering with the following abstract:

The Kalbach-Mann systematics has been improved for the application to reactions induced by 14 MeV neutrons. On the basis of their approach, new parameters for nucleon emission reactions are derived from the Legendre polynomials fitting to the 18 and 25 MeV (p,n) data and the 18 MeV (p,p') data. For α particle emissions, separate parameterizations are performed for equilibrium and preequilibrium components: the Legendre coefficients obtained from the Hauser-Feshbach calculations are parameterized for the former and the same procedure as that of nucleon emissions is applied to the latter. The angular distributions calculated using the present parameters show good agreement with those for 14 MeV (n,n'), (n,p), and (n,α) reactions.

V-A-4

Incident Energy Dependence of Preequilibrium Process in Nucleon-Induced Reactions

Y. Watanabe, K. Kodaka, Y. Kubo, N. Koori, M. Eriguchi, M. Hanada, and I. Kumabe

A paper on this subject was presented at the 1988 Seminar on Nuclear Data, Tokai, Dec.8-9, 1988 with the following abstract:

Proton energy spectra from (p,xp) reactions on ^{98}Mo and ^{106}Pd have been measured at incident energies of 12, 14, 16, and 18 MeV to investigate the incident energy dependence of preequilibrium process. The spectra were compared with a calculation based on the exciton model in which the squared average transition matrix element $|M|^2$ was assumed to be $KA^{-3}E^{-1}$ and isospin conservation was taken into account. The calculated spectra using a constant K-value were in good agreement with all the measured ones. Proton spectra from the ^{54}Fe(p,xp) reaction at 29 and 39 MeV and (n,xn) spectra for several target nuclei at 14-26 MeV were also analyzed by the exciton model to examine the application of the model and the parameters used to the reactions induced by 10-40 MeV nucleon.

V-A-5

Continuum Spectra of 18 MeV (p,p') and (p,n) Reactions on Zr and Pd Isotopes

Y. Watanabe, Y. Kubo, K. Kodaka, N. Koori, M. Eriguchi,

M. Hanada, and I. Kumabe

In order to study preequilibrium process in nucleon induced reactions, energy spectra of protons emitted from (p,p') scattering were measured for $^{90,91,92,94}Zr$ and $^{106,108,110}Pd$ at an incident energy of 18 MeV. The experimental procedure has been described in detail elsewhere.[1] Since experimental data[2] on neutron spectra from 18 MeV (p,n) reactions for the same target nuclei are available, both (p,p') and (p,n) spectra were simultaneously analyzed in terms of the one- and two-component exciton models[3,4,5]. In the analysis, we took the isospin conservation into account and have mainly investigated the dependence of K-value, which is an adjustable parameter used in an empirical relation $|M|^2=KA^{-3}E^{-1}$ for the square of average two-body matrix element, on the nature of emitted nucleon.

From the analysis using the one-component exciton model, it was found that both (p,p') and (p,n) spectra are reproduced well by the calculation using the same K-value if Q-factor[4] is employed as the correction factor for the distinguishibility of proton and neutron degrees of freedom.

The result of the two-component exciton model calculation indicated that relative yields for proton and neutron emissions depend strongly on relative probabilities of exciting proton and neutron in a nucleus in the transition process from one-particle

(1p) states to two-particle and one-hole (2p-1h) states. The calculated (p,p') and (p,n) spectra showed good agreement with the experimental ones if the assumption of equal probability is made. Comparisons between the experimental and calculated spectra for ^{91}Zr and ^{94}Zr are shown in Fig.1.

In addition, the two-component model calculation was applied to neutron induced reactions. The results calculated using the same K-value as the proton induced reactions showed overall agreement with the experimental 14 MeV (n,n') and (n,p) spectra for Nb and In.

References

[1] Y. Watanabe et al., Phys. Rev. C 36, 1325 (1987).

[2] W. Scobel et al., Lawrence Livermore National Laboratory Report No. UCID-20101 (1984).

[3] C. Kalbach, Phys. Rev. C 33, 816 (1986).

[4] S.K. Gupta, Z. Phys. A 303, 329 (1981).

[5] J. Dobes and E. Betak, Z. Phys. A 310, 329 (1983).

[6] C. Kalbach, Z. Phys. A 283, 401 (1977).

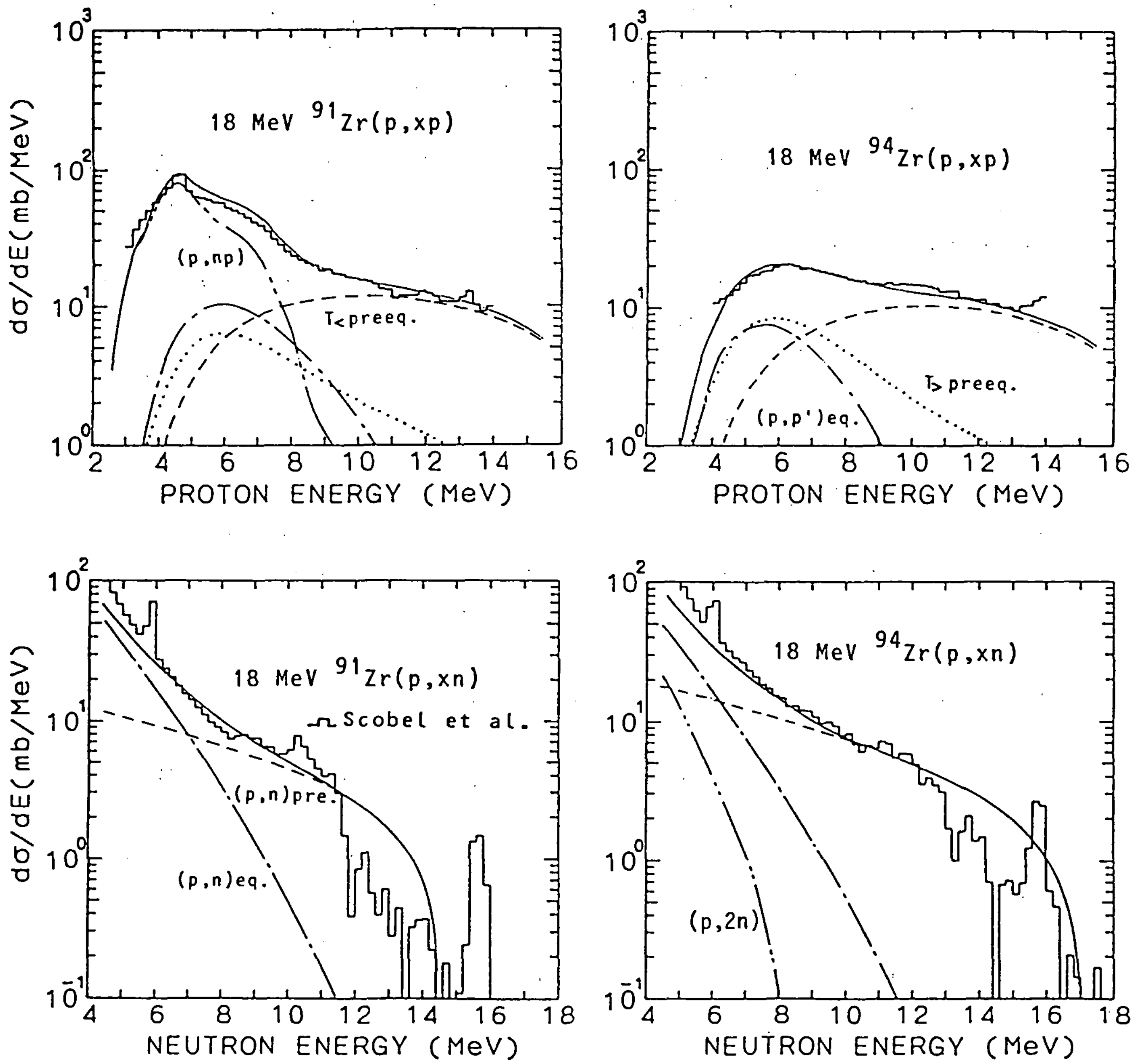

Fig.1 Comparisons between experimental energy spectra and those calculated using the two-component exciton model for 18 MeV (p,p') and (p,n) reactions.

V-A-6

SPALLATION REACTION CALCULATION TO IMPROVE EMISSION YIELDS OF HIGH ENERGY NEUTRONS IN THE BACKWARD DIRECTION

Kenji Ishibashi and Akira Katase+

The computer program[1] of Nucleon Meson Transport Code (NMTC) or High Energy Transport Code (HETC) has been utilized for the engineering purposes in the region of incident energy above 100 MeV. These codes employ the intranuclear-cascade-evaporation model by the Monte Carlo method. It is well known that the codes systematically underestimate the yields of high energy neutrons which are emitted into the backward direction.

For intranuclear nucleons, the program assumes the Fermi gas model at zero temperature. On the other hand, intranuclear nucleons with very high momentum[2] have been used in the analysis of proton emission into the backward direction. Presence of these high-momentum nucleons leads to increase in the yields of high energy proton in this direction.

Such nucleons with high momentum are introduced into HETC in this study. The momentum distribution is the same as in reference 2. In the usual HETC, the calculation at the intranuclear-cascade stage is terminated by a constant cut-off energy E_c. Unlike this situation, a probability density distribution function $f(E_c)=f_0\,(1-E_c/E_0)$ is used in this study to determine the end of cascade stage. The results are shown in Figs. 1 and 2 for thin-target experiments.[3,4] Solid lines indicate the results of the present calculation. Dashed lines stand for the standard HETC calculation. The yields of the high-energy backward neutron emission are considerably improved. Besides, the shoulders of the experimental spectra in the energy of 20-40 MeV are reproduced better by the solid than by dashed lines.

References

1) T.W. Armstrong et al.: Nucl. Sci. Eng. **49** (1972) 82.
2) Y. Haneishi and T. Fujita: Phys. Rev. C **33** (1986) 260.
3) S. Cierjacks et al.: Phys. Rev. C **36** (1987) 1976.
4) M.M. Meier et al.: Radiation Effects **96** (1986) 1415.

+Faculty of engineering, Tohwa University
Chikusigaoka, Minami-ku, Fukuoka 812.

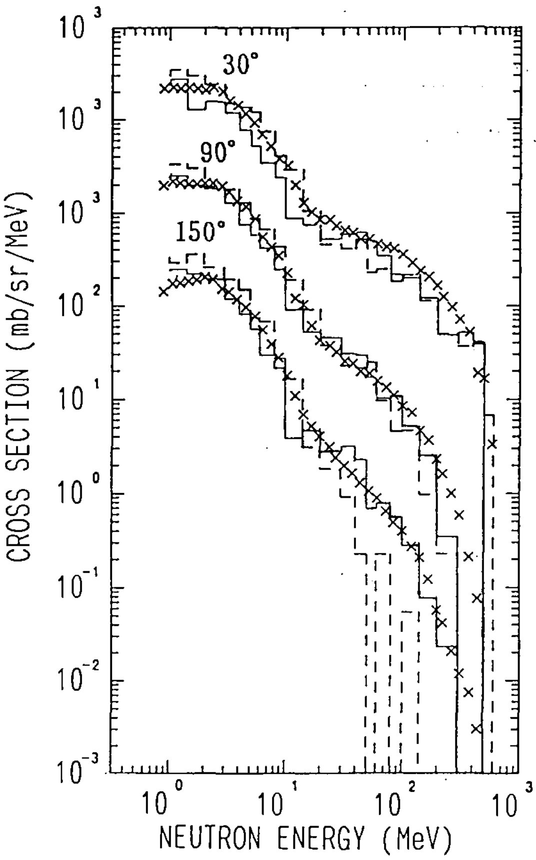

Fig. 1. Neutron emission cross section for the incidence of 585 MeV protons on lead. Marks of cross indicate experimental results.[3] Solid and dashed lines shows calculation results by the present and standard HETC, respectively.

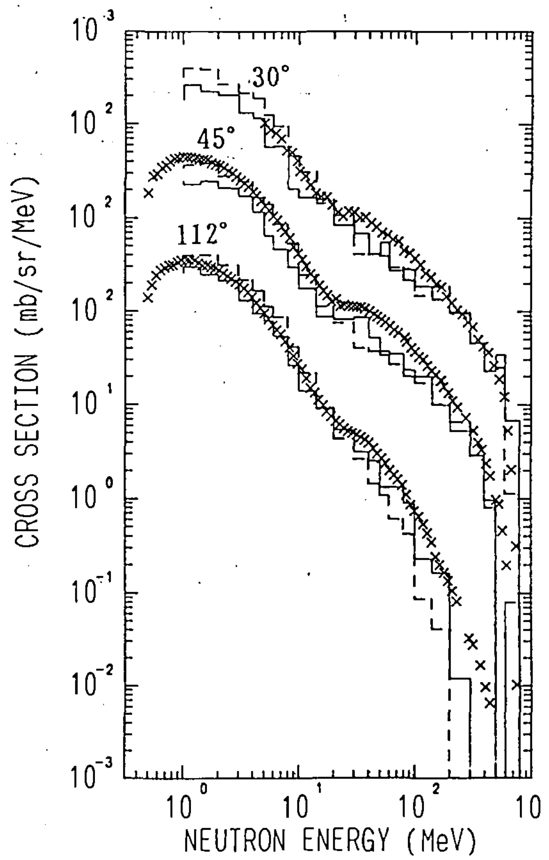

Fig. 2. Neutron emission cross section for the incidence of 800 MeV protons on lead. Marks of cross indicate experimental results.[4] Solid and dashed lines shows calculation results by the present and standard HETC, respectively.

B. Energy Conversion Engineering
Interdisciplinary Graduate School
of Engineering Sciences

V-B-1 EVALUATION OF $^{238}U(n,n')$ CROSS SECTIONS

Y. Uenohara and Y. Kanda

Inelastic cross sections of ^{238}U are very important quantities for design of fast breeder reactors. The previous evaluation, JENDL-2, of inelastic cross sections for discrete levels were inaccurate above neutron energy of 3 MeV because of lack of experimental data. Recently, the inelastic cross sections for some discrete levels have been measured above neutron energy of several MeV. These experimental data are larger than JENDL-2.

In the present evaluation, the coupled channel model code ECIS and DWBA code DWUCK4 are used for the calculations of direct reaction components for the discrete levels. The compound nucleus reaction components are done by using the statistical model code CASTHY. The (n,n') cross sections for the twenty six discrete levels and continuous region are included.

V-B-2

ADJUSTMENT OF EVALUATED FISSION NEUTRON SPECTRUM BY INTEGRAL DATA

Toshihiko KAWANO, Yuji UENOHARA, and Yukinori KANDA

Fission spectra of both Madland-Nix's ^{235}U [1] and Mannhart's ^{252}Cf [2] are adjusted by Bayesian method, so that integral data are consistent with differential data. Six cross sections, $^{27}Al(n,p)$, $^{27}Al(n,\alpha)$, $^{54}Fe(n,p)$, $^{56}Fe(n,p)$, $^{59}Co(n,\alpha)$ and $^{58}Ni(n,p)$, are chosen for the bases of adjustment procedure. An effect of an *a priori* covariance matrix is also examined. Correlation factors between different energy points are assumed to be nothing in one case and all 50 % in another case.

The spectra are reduced dominantly at the neutron energy of from 3 MeV to 15 MeV where the differential data are effective.

Differential cross sections averaged by Mannhart's spectrum are consistent with the experimental integral values, and a variance is small.

There are little difference of the *a posteriori* spectra between the case of 0 % correlation assumption and the case of 50 %.

This study was published in JAERI-M89-026, 275(1989)

REFERENCES

1) JENDL Compilation Group (Nuclear Data Center,JAERI):JENDL-3T Private Communication (1987).

2) W.Mannhart, "Evaluation of the Cf-252 Fission Neutron Spectrum between 0 MeV and 20 MeV", 6th ASTM/Euratom Symposium on Reactor Dosimetry, Jackson Hole, Wyoming USA, June 1987.

VI. NAGOYA UNIVERSITY

A. Department of Nuclear Engineering

Faculty of Engineering

VI-A-1

Measurement of formation cross sections of short-lived nuclei by 13.4-14.9 MeV neutrons

T. Katoh, K. Kawade, H. Yamamoto, *T. Iida and *A. Takahashi

Neutron activation cross sections of short-lived nuclei with half-lives between 0.5 and 20 min have been measured at neutron energy of 13.4 to 14.9 MeV by the activation method for 32 reactions; ^{14}N(n,2n), ^{26}Mg(n,α), ^{27}Al(n,p), ^{28}Si(n,p), ^{30}Si(n,α),(n,n'p), ^{31}P(n,2n),(n,α), ^{37}Cl(n,p), ^{51}V(n,p), ^{52}Cr(n,p), ^{53}Cr(n,p),(n,n'p), ^{54}Fe(n,2n)^{g}, ^{55}Mn(n,α), ^{62}Ni(n,p)^{m,g}, ^{66}Zn(n,p), ^{67}Zn(n,n'p), ^{68}Zn(n,p), ^{63}Cu(n,2n), ^{65}Cu(n,α)^{m}, ^{88}Sr(n,p), ^{90}Zr(n,2n)^{m}, ^{94}Zr(n,p), ^{92}Mo(n,2n)^{m,g},(n,α)^{m}, ^{97}Mo(n,p)^{m}, ^{98}Mo(n,n'p)^{m}, and ^{113}In(n,2n)^{m,g}.

Experiments were performed at the Intense 14-MeV-Neutron Source Facility (OKTAVIAN) of Osaka University. For the activation of samples, pneumatic tubes were set at 6 directions (between 0° and 155°) for the incident deuteron beam direction. The amount of activities of some positron emitting nuclei which emitted nearly no gamma-ray was obtained from the intensities

---

* Department of Nuclear Engineering, Osaka University,

of the annihilation gamma-rays of 511 keV. The annihilation radiations were measured by setting the irradiated samples between two 10 mm thick acrylic plates. The broadening of gamma emitting points in the plates was examined by using the 514 keV gamma-ray from ^{85}Sr. The effect of broadening can be neglected for the positron energies less than 3 MeV, within the experimental errors of about 1 %. The neutron energies were determined by the Zr/Nb method. The errors are estimated to be less than 100 keV. The neutron flux at the irradiation points was monitored by using two aluminum foils (purity: 99.2 %, 1 cm x 1 cm x 0.2 cm). The reference reaction for the flux measurement was the $^{27}Al(n,p)^{27}Mg$(9.46 min) reaction, which was determined referring to the standard $^{27}Al(n,\alpha)^{24}Na$ reaction (ENDF/B-V).

Corrections were made for time fluctuation of neutron flux, thickness of samples, self absorption of γ-ray, sum-peak effect of γ-ray and contribution of low energy neutrons below 10 MeV. Accuracies of the obtained cross-sections were around 4 % in case of the good statistics.

A part of this work was presented at the 1988 Seminar on Nuclear Data, and published in JAERI-M 89-026.

VII. Rikkyo (St. Paul's) University

A. Department of Physics

Faculty of Science

VII-A-1

Measurements of Differential Cross Sections for the Reactions $^{6,7}Li(n,d)^{5,6}He$ and $^{6,7}Li(n,t)^{4,5}He$

S. Shirato, S. Shibuya, K. Hata, Y. Ando and K. Shibata*

A paper on this subject has been presented as JAERI-M 89-107.

Abstract

A summary of our measured cross sections for 14.1 MeV neutron-induced reactions on lithium isotopes has been presented. Our data were measured with two counter telescopes, each of which consisted of two gas proportional counters and silicon ΔE and E detectors. Measured energy spectra of deuterons and tritons from $^{6}Li(n,d)n^{4}He$ and $^{7}Li(n,t)n^{4}He$, respectively, were analyzed by a simple final-state interaction theory. Measured angular distributions for these reactions as well as $^{6}Li(n,t)^{4}He$ and $^{7}Li(n,d)^{6}He$ were analyzed by exact finite-range distorted wave Born approximation (EFR-DWBA) calculations. Spectroscopic factors extracted from the EFR-DWBA analyses of our data have been compared with various theoretical predictions.

---

* Japan Atomic Energy Research Institute

VII-A-2

Absolute Determination of T-d Neutron Yields by the Associated Particle Method

S. Shirato, S. Shibuya, Y. Ando, T. Kokubu* and K. Hata

This paper has been published in Nucl. Instr. Methods A278, 477 (1989) with the following abstract.

T-d neutron yields have been determined with a high accuracy of about 1% by measuring the associated α-particles from the $^3H(d,n)^4He$ reaction using a ^3H-Ti-Cu solid target at selected incident deuteron energies in the range 140 - 300 keV. Our results on the determination of the neutron yield as well as the neutron fluence rate at a certain position far from the neutron source point are presented. The T-d neutrons were produced by the 300 kV Cockcroft-Walton accelerator of Rikkyo University. We used a silicon p-i-n photodiode as an α-particle detector for the yield determination and a NE213 liquid scintillator (2 in. x 2 in.) or a counter telescope with a $(CD_2)_n$ radiator as a neutron detector for the fluence rate determination. A collimator with a hole of different size (2, 3 or 4 mm in diameter) was placed in front of the α-particle detector to define precisely the solid angle. The results on the neutron yields obtained by both methods are compared and discussed. The time characteristics of the neutron detector have also been studied using both the associated α-particle detectors of the silicon photodiode and the NE102A thin (10 μm) plastic scintillator.

---

* Hitachi Seisakusho Co.

VII-A-3

Search for Neutron Emission from Cold D-d Fusion in Electrochemical Experiments

K. Hata, Y. Ando, H. Murakami, K. Ieki, N. Iwasa,
S. Shirato, K. Sekine* and T. Takamura*

We preliminarily measured neutrons in both cases with and without an electrochemical straight-tube type cell of a electrolyte of heavy water D_2O and heavy sulfuric acid D_2SO_4 (1 N) by using three neutron detectors. Two of the neutron detectors are NE213 liquid scintillators of 2 in. thick by 2 in. diameter and of 30 cm thick by 10 cm diameter, operating under the best condition of the n-γ discrimination. The other neutron detector is a BF_3 counter. These detectors were calibrated by measuring D-d neutrons provided by a Cockcroft-Walton accelerator as well as by neutrons from a Ra-Be source. These neutron detectors and a NaI(Tl) counter for γ-detection were positioned close (almost contact) to the cell operating with a cathode of Pd (5.0 mm x 23.5 mm = 0.461 cm^3; 5.598 g in 99.98 % purity) and an anode of Pt, between which the current was 300 mA.

The data of neutrons and γ-rays from 4 to 10 June, 1989 were taken in list mode by the CAMAC system. During this run, measurements of background were performed before and after electrolysis operation of the cell. The data were analyzed event by event in off-line, and the time evolution of the neutron counts over periods of 100 minutes was obtained.
A part of the result for the case of observation using the

2 in. x 2 in. NE213 neutron detector is shown in fig. 1. The maximum counting rate was found to be 0.7 ± 0.1 neutrons /cm^3sec (the term "cm^3" refers to the volume of Pd cathode), which was in accidental agreement with a neutron production rate reported by Jones et al.[1] However, because the background level is relatively high as seen in fig. 1, it is appropriate to say that we could not observe cold nuclear fusion within background statistics in this preliminary experiment. A careful comparison was made between our data and the data of current cosmic-neutron measurements using BF_3 counters.

Reference

1) S. E. Jones, E. P. Palmer, J. B. Czirr, D. L. Decker, G. L. Jensen, J. M. Thorne, S. F. Taylor and J. Rafelski, Nature (London) 338, 737 (1989).

---

* Department of Chemistry, Rikkyo University

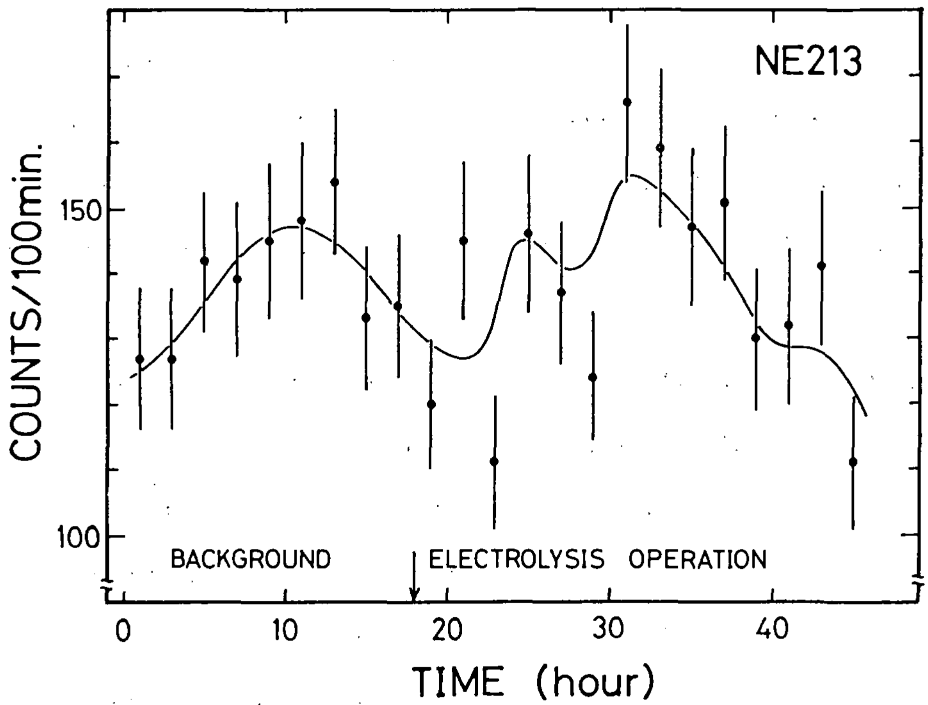

Fig. 1. Time evolution of neutron counts during early days (4 - 10 June, 1989).

VIII Tohoku University

A. Department of Nuclear Engineering

Faculty of Engineering

VIII-A-1

Measurement of Prompt Fission Neutron Spectrum of ^{238}U for 2-Mev Incident Neutrons

M.Baba, H.Wakabayashi, N.Ito, K.Maeda and N.Hirakawa

The prompt fission neutron spectra of ^{238}U have been measured for 2-MeV incident neutrons, at two emission angles of 90- and 135-deg., using Tohoku university Dynamitron TOF spectrometer.

The primary neutrons were produced by the T(p,n) reaction on a solid tritium target with the energy spread of 80 keV. The fission sample was a solid cylinder of elemental uranium, 2cm in dia. and 5 cm long. The fission neutrons were detected by a massively shielded NE213 scintillator, 14cm in dia. and 10cm thick, coupled to fast timing electronics and gamma-ray rejection circuits. The flight path was 3.86 m long, and the overall timing resolution was about 1.5 ns. Cares were taken for reduction of time-dependent backgrounds by use of tight collimation and optimum detector bias.

In the data reduction, the following effects were taken into consideration; 1)sample-dependent backgrounds as well as sample-out ones, 2)multiple-scattering of fission neutrons in the sample, and 3)finite energy resolution of the spectrometer. Figure 1 shows the result at 135-deg.. The resulting spectra were fitted with Maxwellian and Watt type distribution functions;

$N_M(E) = C_M E^{1/2} Exp(-E/Tm)$;Maxwellian distribution,

$N_W(E) = C_W Exp(-E/A) Sinh(BE)^{1/2}$;Watt type distribution,

where E and Tm are the neutron energy and Maxwellian temperature, respectively.

The parameter values and their errors obtained by the fit are as follows:

Tm = 1.24±0.01, A = 0.98±0.02, B = 2.00±0.10 ; 90-deg,

Tm = 1.26±0.01, A = 0.98±0.02, B = 2.09±0.09 ;135-deg..

The result at 90-deg. shows a slightly softer spectrum and a smaller yield (about 5%) of fission neutrons, compared with those at 135-deg.; this result will be interpreted by assuming the anisotropy of fission fragments with respect to the incident beam axis.

A short report is presented in JAERI-M 89-026 pp.253, and a full report is now in preparation.

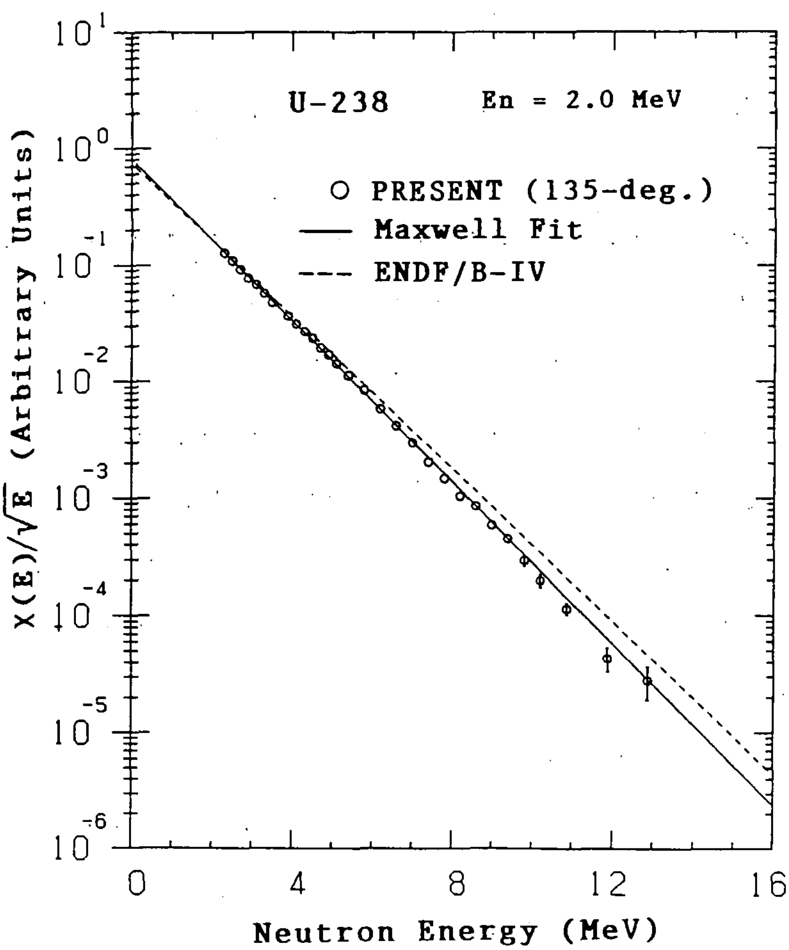

Fig.1 Fission neutron spectrum of U-238 at 2 MeV incident energy and emission angle of 135-deg., divided by square root E.

VIII-A-2

Double-differential Neutron Emission Spectra of ^{238}U and ^{232}Th for 1.2, 2.0, 4.2, 6.1 and 14.1 MeV Neutrons

M.Baba, H.Wakabayashi, N.Ito, K.Maeda and N.Hirakawa

We have measured the neutron emission spectra for fast neutron interaction with ^{238}U and ^{232}Th using Tohoku university Dynamitron TOF spectrometer, at 6 to 8 scattering angles between 30- and 150-deg., except for 1.2 MeV where measurements were made at two angles of 45 and 120-deg..

The primary neutrons were obtained via the T(p,n), D(d,n) and T(d,n) reactions for measurements at 1.2 & 2.0, 4.2 & 6.1, and 14.1 MeV, using solid tritium and gaseous deuterium targets. The scattering samples were metallic cylinder of elemental uranium and thorium, 2cm in dia. and 5cm long. The scattered neutrons were detected by a NE213 scintillator, 14cm in dia. & 10cm thick for 14 MeV measurements and 5" in dia. and 2" thick for MeV region measurements. The flight path length was around 5m.

The data were corrected for the effects of 1)backgrounds including sample activity, 2)finite sample size, and 3)parasitic and degraded components in source neutrons.

Figure 1 shows the examples of angle-integrated emission spectra at 2 and 14 MeV incident energies for each sample, together with the corresponding values derived from ENDF/B-IV. (Note that the experimental values for elastic scattering peak do not include the contribution from the forward angles than 30-deg..) The secondary neutrons at 14 MeV measurements show marked angle dependence, and their angular distributions are described fairly well by Kalbach-Mann systematics[1).]

A short description of the subject is presented in Ref.2. A full paper is now in preparation and will be submitted for publication.

References:

1. C.Kalbach and F.M.Mann, Phys. Rev., C11(1981) 112

2. M.Baba et al., JAERI-M 89-026 pp.253, and

NETU-51 (Dep. Nucl.Eng., Tohoku University 1989) pp.18.

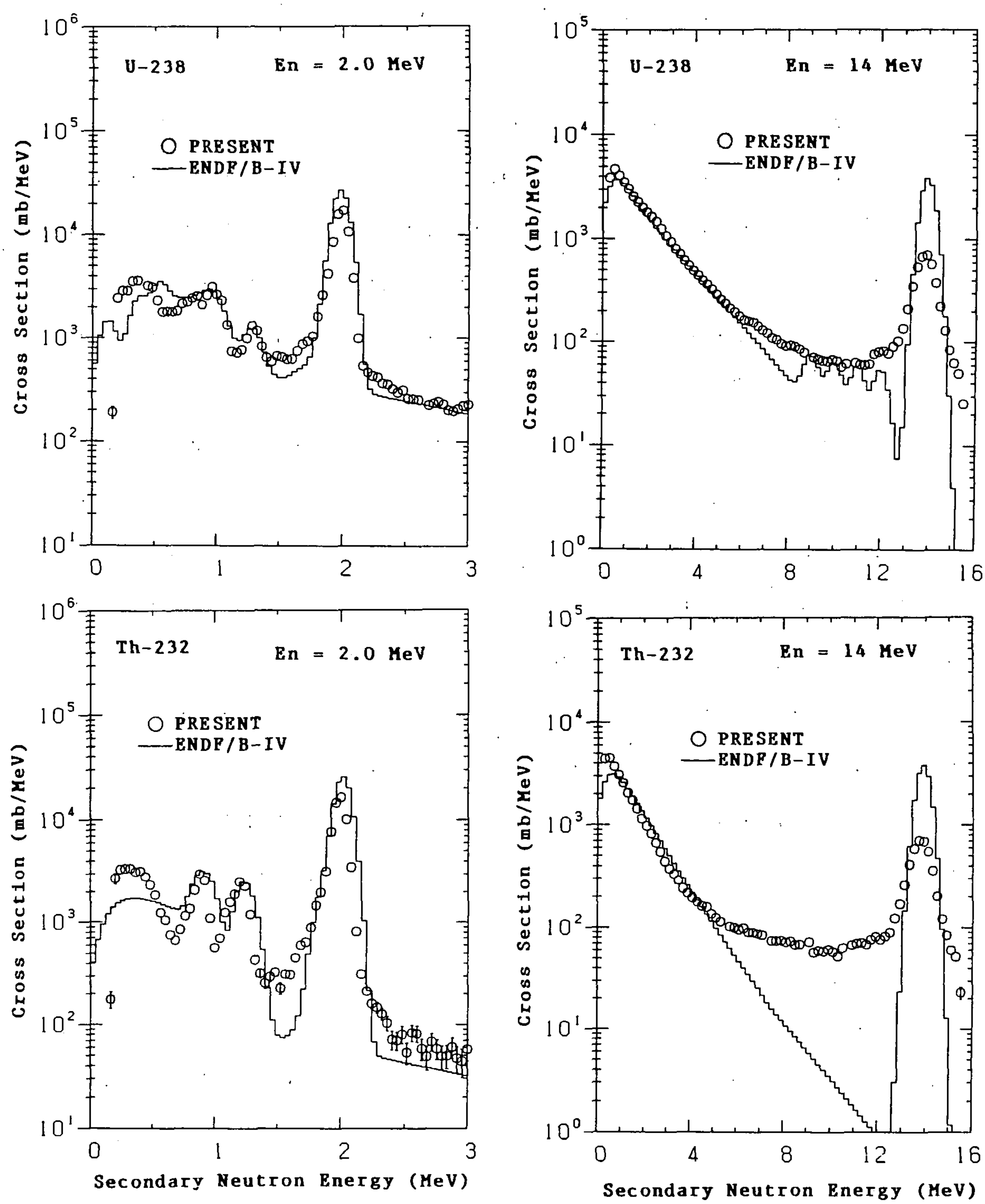

Fig.1 Angle-integrated neutron emission spectra from U-238 and Th-232 at incident energies of 2 MeV and 14 MeV.

VIII-A-3

A Post-Acceleration Beam Chopper for 4.5MV Dynamitron Neutron Generator

S.Matsuyama, M.Fujisawa, M.Baba, T.Iwasaki, S.Iwasaki

R.Sakamoto, N.Hirakawa and K.Sugiyama

A post-acceleration beam chopping system (PACS) was installed for Tohoku university 4.5 MV Dynamitron accelerator which has been used for pulsed neutron generation in fast neutron time-of-flight (TOF) works. The aim of the PACS is to improve the energy resolution in TOF experiments by eliminating a wing and reducing the duration of the beam pulse provided by the terminal pulser.

PACS shortens the duration of pulsed beam by sweeping the accelerated beam pulse across a chopping slit with a deflector, 50 cm long with 2.5 cm spacing and driven by 8 MHz R.F (10 kV p-p max.). The system is useful also for reduction of dark current and spurious components in the pulsed beam. High voltage R.F is provided by a tank circuit driven by a commercial wide band linear amplifier; this method is advantageous because of minimum number of high voltage items, and simple tuning and maintenance. Synchronization of PACS with the beam is realized by triggering the amplifier with the beam pickoff signal with phase adjustment.

After installation, PACS has been applied successfully for measurements of neutron scattering cross sections and emission spectra. Figure 1 shows an example of emission spectrum data from polyethylene sample for 14.1 MeV incident neutrons measured using PACS. The operation of PACS improves the energy resolution remarkably; the separation between the peaks due to the scattering from hydrogen and carbon becomes much clear by PACS. Thus the PACS is thought effective especially for study of scattering cross sections of closely-spaced levels and now applied for double-differential neutron emission cross sections studies.

The design and construction of the system is described in Ref.1 and 2.

References:

1. S.Matsuyama et al., NETU-50 (Dep.Nucl.Eng., Tohoku Univ., 1988) pp.6

2. S.matsuyama et al., NETU-51 (1989) pp.6

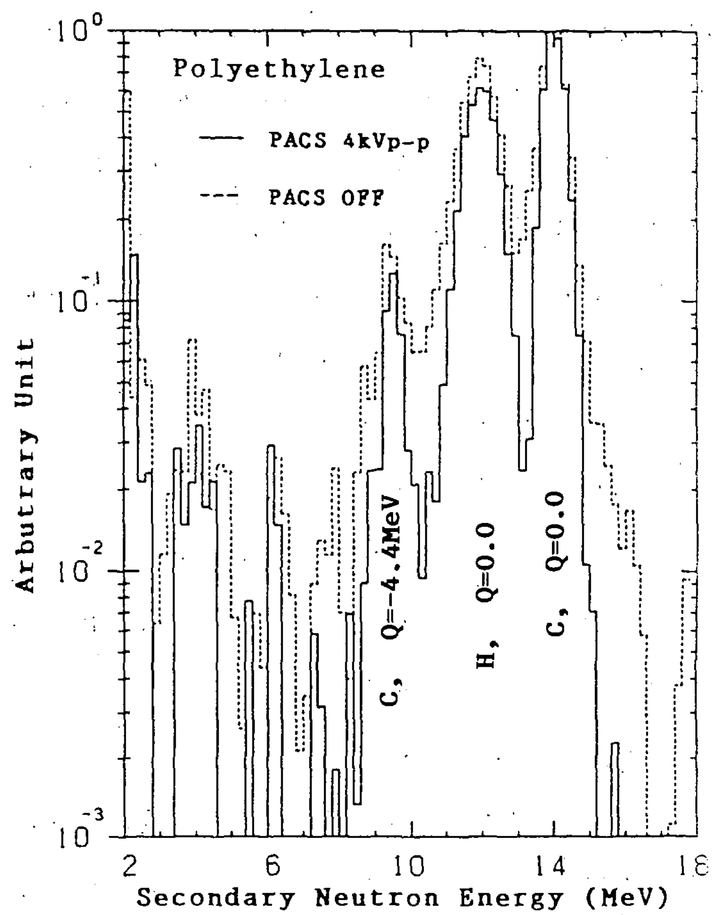

Fig.1 Neutron emission spectra from scattering of 14.1 MeV neutrons by a polyethylene sample at scattering angle of 25-deg.; the data with PACS on are compared with those for PACS off.

VIII-B-1 Activation Cross Section Measurements by 15-35 MeV Quasi-Monoenergetic p-Be Neutrons

Nakamura T., Kondo Y., Sugita H. and Uwamino Y.*

1. Quasi-monoenergetic neutrons

The experimental data on neutron activation cross sections are limited to the neutron energy lower than 20 MeV in general, except for several reactions. This may be because of the lack of the intense monoenergetic neutron beam of energy higher than 20 MeV. We have developed a quasi-monoenergetic neutron beam of energy from 15 MeV to 35 MeV by the Be(p,n) reaction, with changing the proton energy from 20 MeV up to 40 MeV.[1)]

The beryllium target of 1 or 2 mm in thickness backed by the cooling water was bombarded through a 20-mm diam carbon collimator by a proton beam from a cyclotron. The neutron energy spectra at 0 degree to the proton beam were measured with a NE-213 scintillator for proton energies of 20, 22.5, 25, 27.5, 30, 32.5, 35, 37.5 and 40 MeV. The neutron spectra unfolded from the measured pulse height distributions are shown in Fig. 1, together with the peak neutron energy 4-5 MeV lower than the proton energy. The spectra indicated pretty good monoenergetic spectra having the energy resolution of about 4 MeV, although they included the contamination of low energy neutron components.

Institute for Nuclear Study, University of Tokyo*

2. Activation cross sections

By using this quasi-monoenergetic neutrons, the activation cross section measurements were performed for target materials of C, Na, Mg, Al, Si, Ca, Ti, V, Cr, Mn, Co, Cu, Zn, Zr, Nb, Mo and Au. These target samples were irradiated by this neutron beam at a position of 20 cm behind the beryllium target.

The activation rates were obtained from the gamma-ray activities of the samples measured by a high purity Ge detector. From the activation rates, we estimated the activation cross sections in the following way; 1) averaging in the energy range from 14 to 39 MeV (named AVERAGE), 2) least square fitting to the values calculated by the ALICE code[2] (PARA), and 3) unfolding by the SAND-2 (SAND2)[3] and NEUPAC (NEUPAC)[4] codes, with the initial guess of the evaluated data or the ALICE calculation. Among of many measured results, we exemplified the following four results.

Figures 2 and 3 give the $^{27}Al(n,\alpha)^{24}Na$ and $^{12}C(n,2n)^{11}C$ cross sections, respectively, obtained from averaging and unfolding by SAND-2 and NEUPAC. Our experimental data are compared with the evaluated data in ENDF/B-5[5] and by Greenwood[6] for $^{27}Al(n,\alpha)$, in 05S[7] for $^{12}C(n,2n)$. Our data estimated from three methods, AVERAGE, SAND2 and NEUPAC agree very well each other and also to the Greenwood's data and 05S data, but the ENDF/B-5 data in the energy range above 14 MeV are a little higher than the others.

Figures 4 and 5 give the $^{nat}Si(n,XnYp)^{28}Al$ and $^{nat}Zn(n,XnYp)^{64}Cu$ cross sections, respectively, obtained from least-square fitting and unfolding. No evaluated cross section data exist for these two reactions, then the ALICE calculation is used as the initial guess of unfolding. Three different methods, PARA, SAND2 and NEUPAC, give very similar cross section values. In Fig. 4, a large peak around 15 MeV corresponds to the

$^{28}Si(n,p)^{28}Al$ cross section due to 92.23% ^{28}Si in ^{nat}Si and a small peak around 26 MeV to the $^{29}Si(n,np)^{28}Al$ due to 4.67% ^{29}Si. Similarly in Fig. 5, a large peak around 10 MeV corresponds to the $^{64}Zn(n,p)^{64}Cu$ cross section due to 48.6% ^{64}Zn in ^{nat}Zn and a small peak around 35 MeV to the $^{66}Zn(n,2np)^{64}Cu$ due to 27.9% ^{66}Zn.

References

1) Y. Uwamino, T. Ohkubo, A. Torii and T. Nakamura, Nucl. Instr. and Meth. A271 (1988) 546.

2) M. Blann and J. Bisplinghoff, LLNL report No. UCID 19614 (1983).

3) W. N. McElroy et al., AFWL-TR-67-41, Vols. 1-4, Air Force Weapons Laboratory (1967).

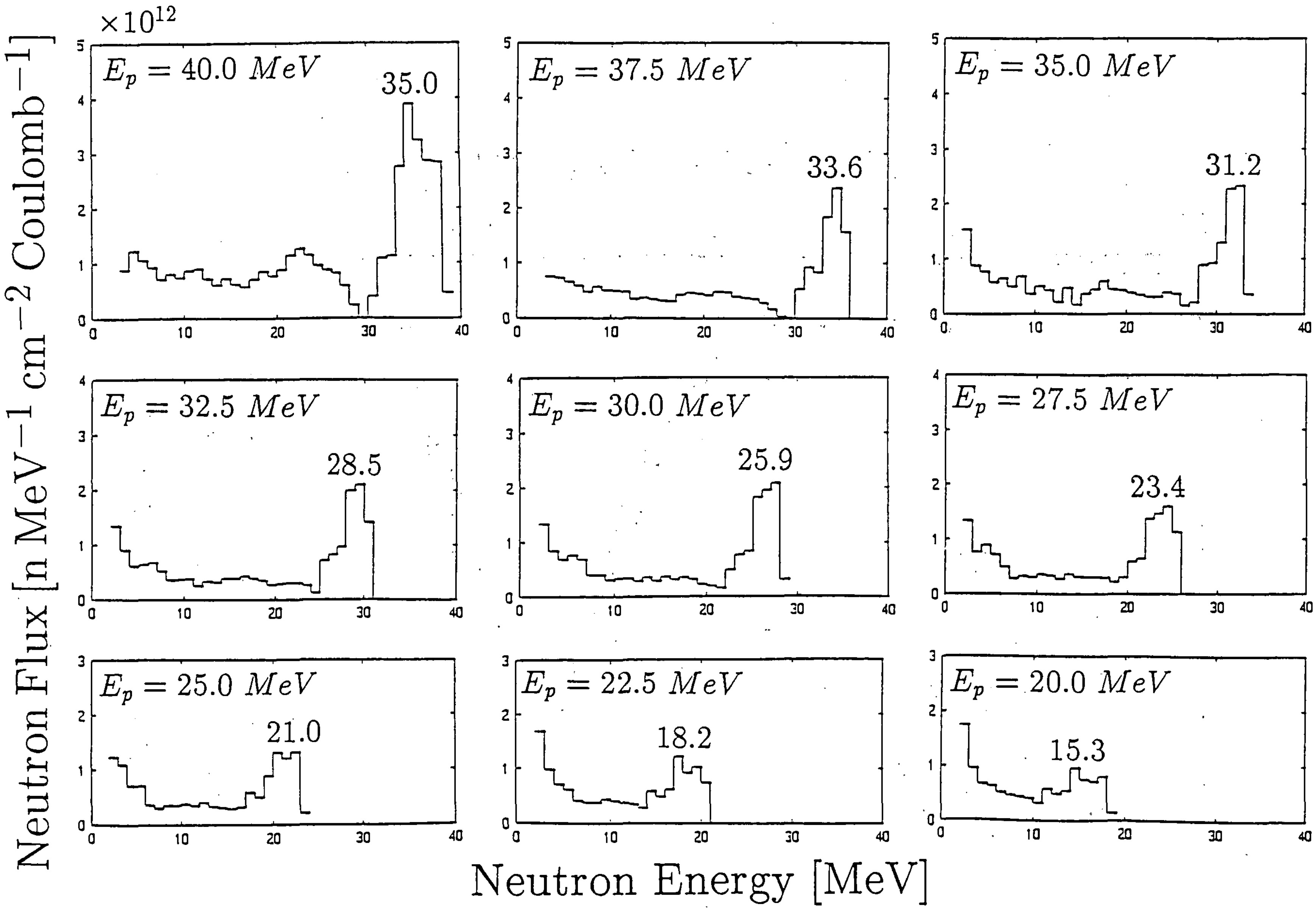

Fig. 1 Quasi-monoenergetic neutron spectra by P-Be reaction

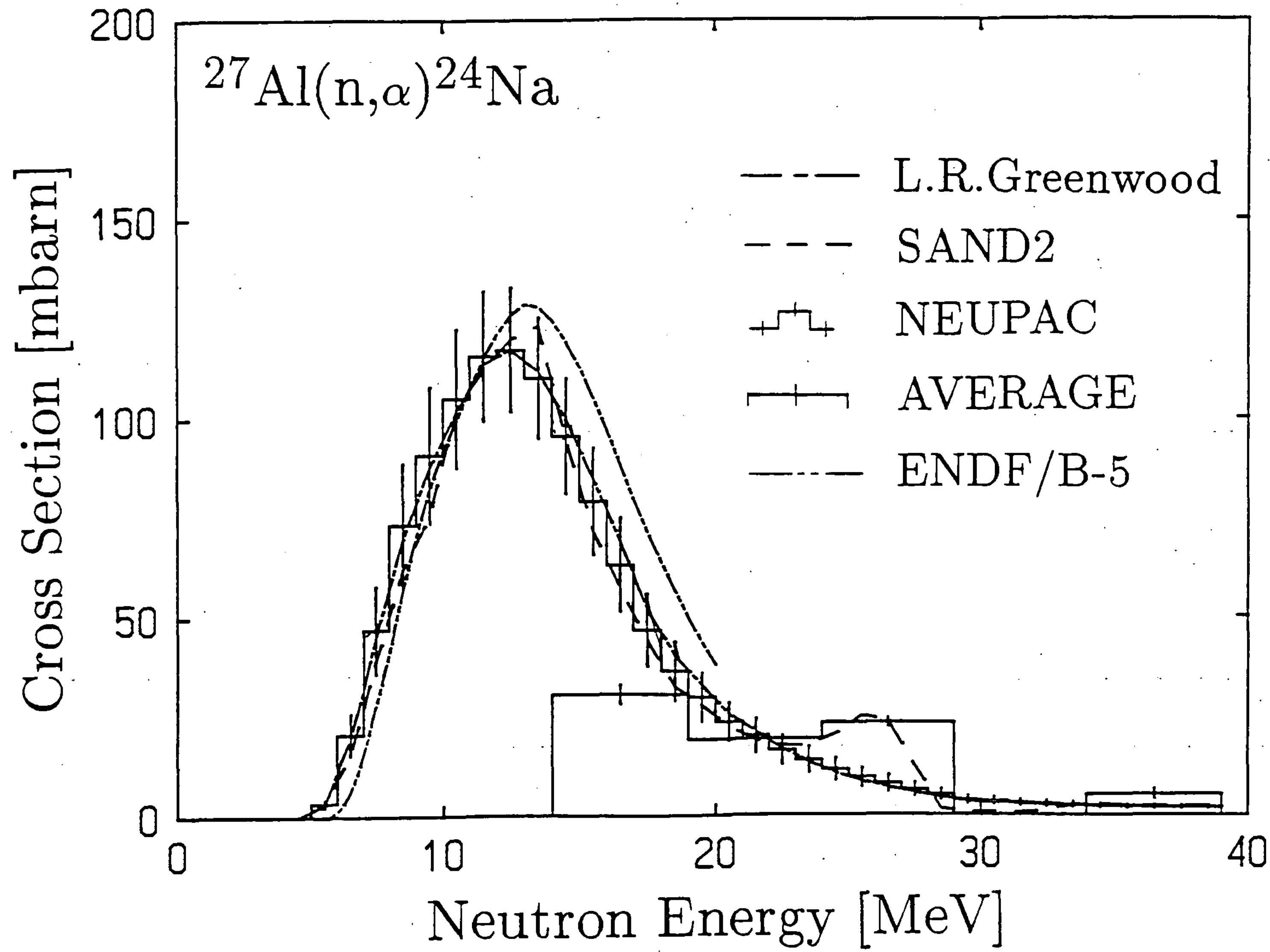

Fig. 2 Excitation function of $^{27}Al\,(n,\ \alpha)\,^{24}Na$ reaction

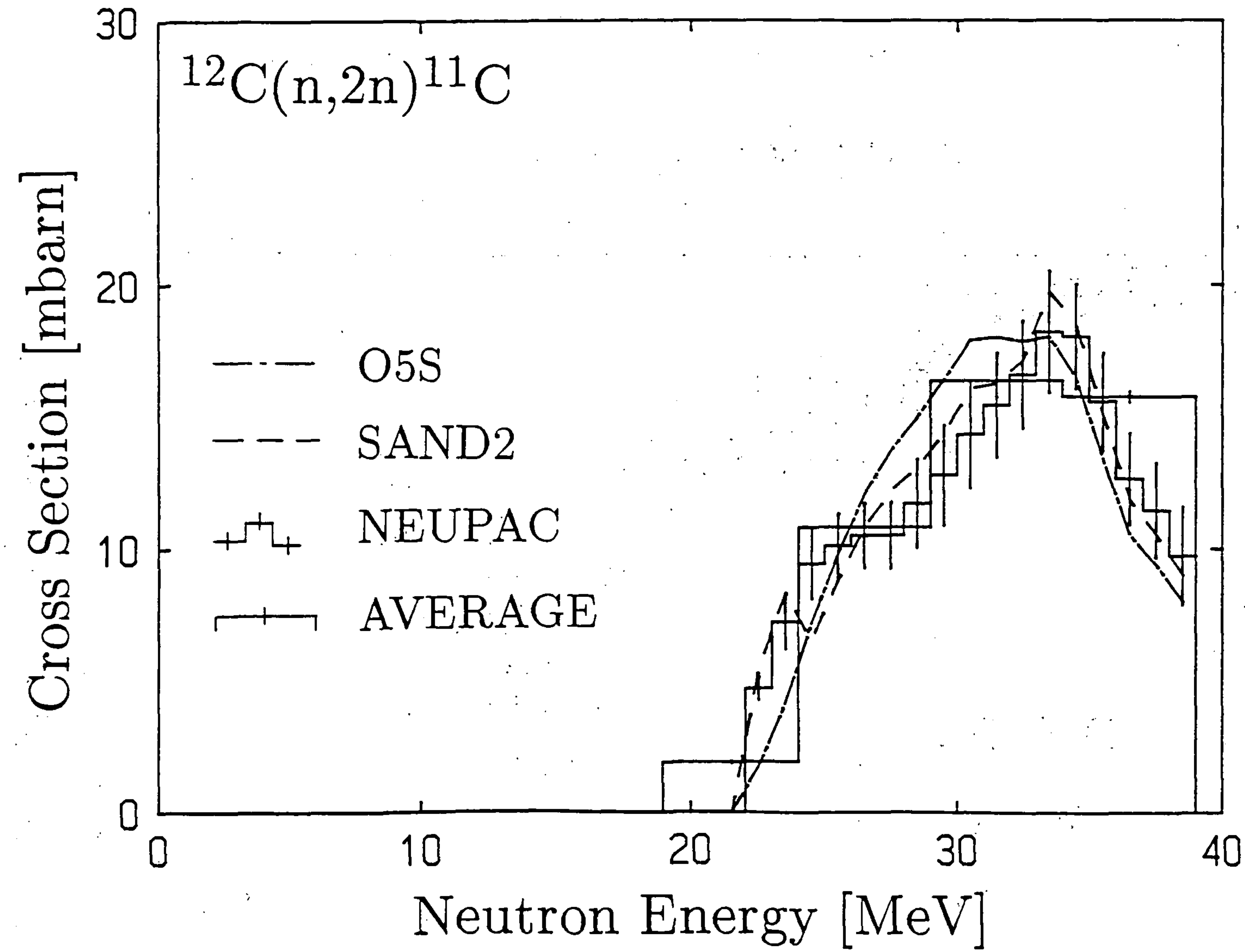

Fig. 3 Excitation function of $^{12}C(n, 2n)^{11}C$ reaction

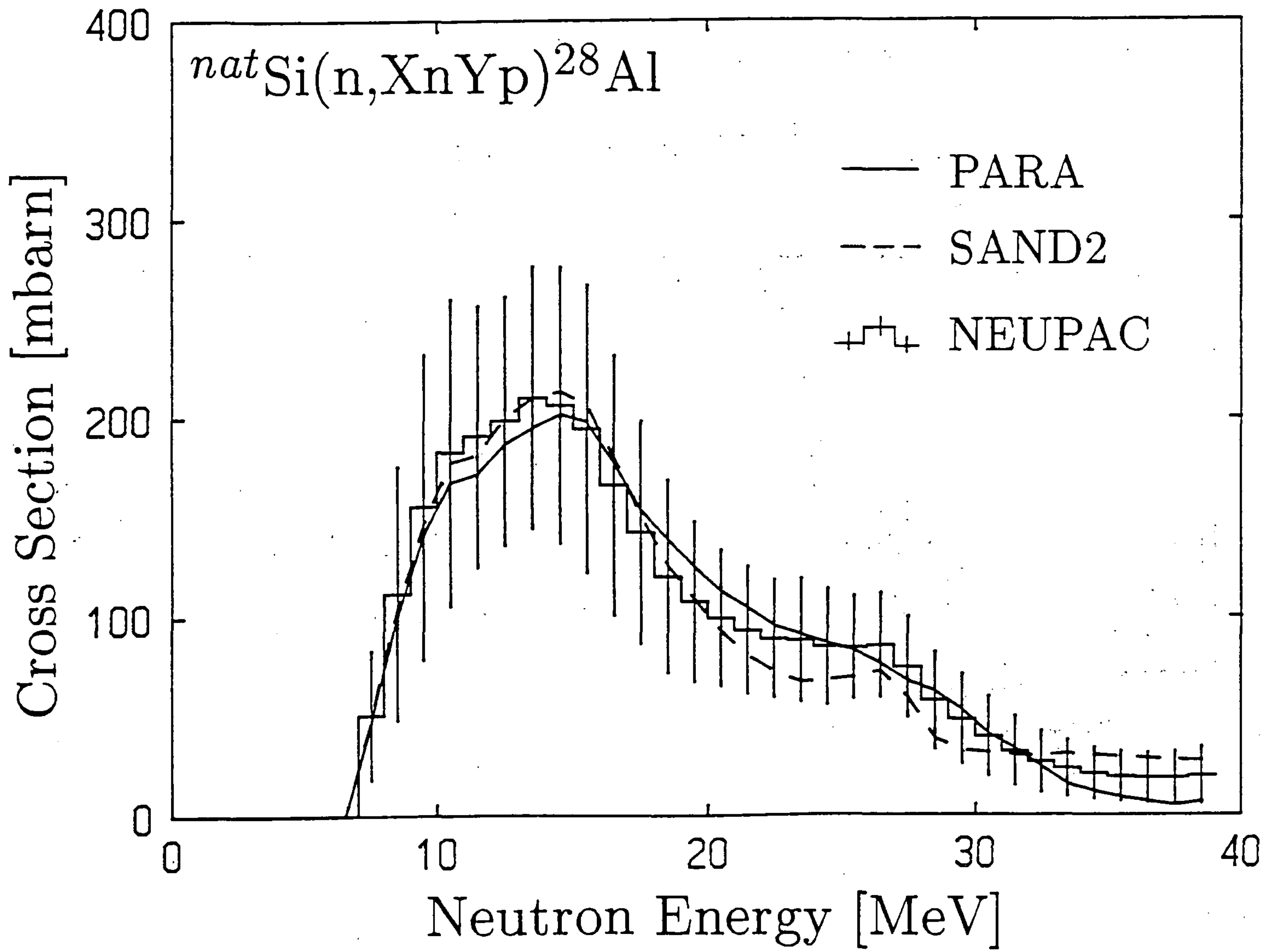

Fig. 4 Excitation function of ^{nat}Si (n, XnYp) ^{28}Al reaction

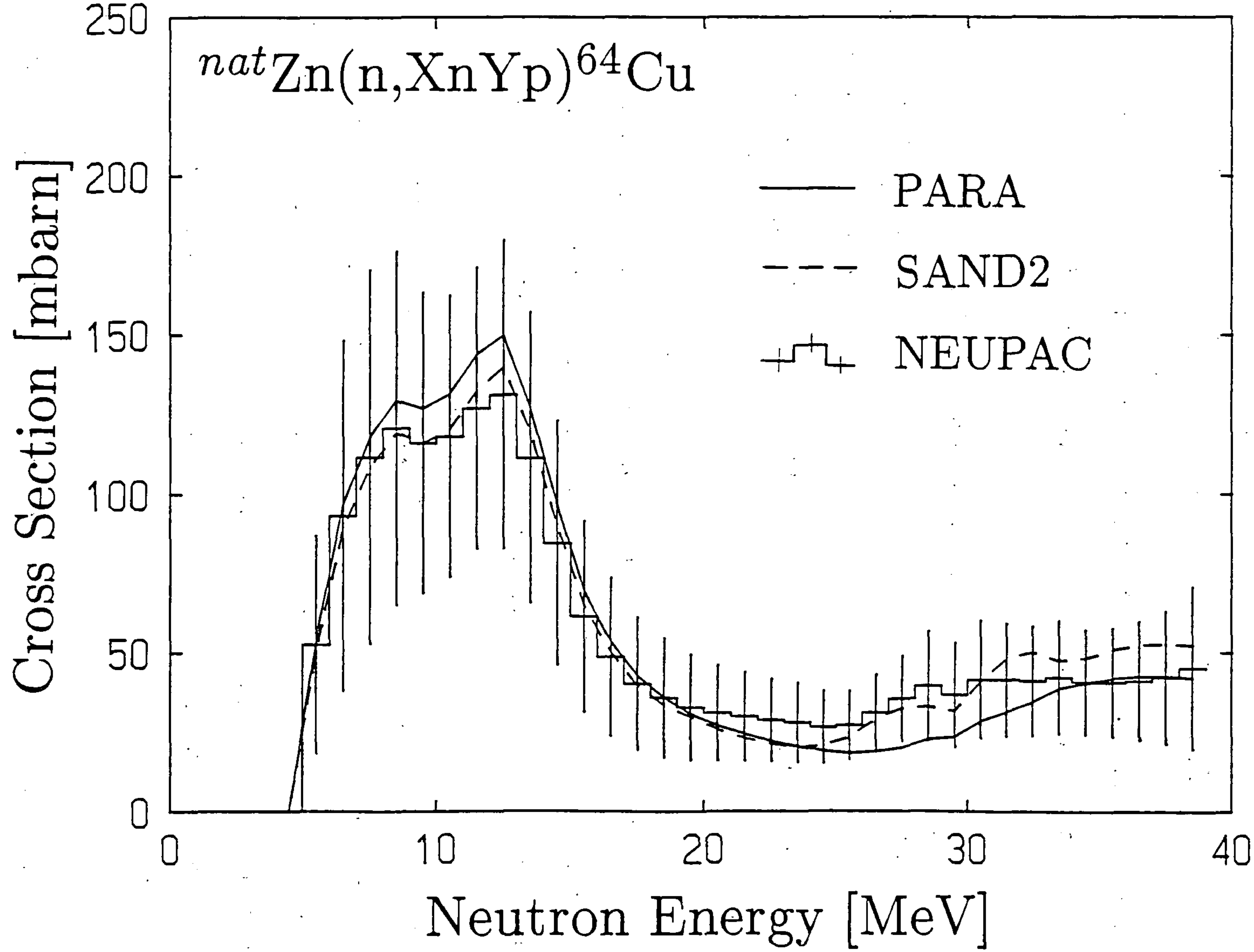

Fig. 5 Excitation function of ^{nat}Zn (n, XnYp) ^{64}Cu reaction

C. Laboratory of Nuclear Science

VIII-C-1 Photopion Production from Nuclei

K.Shoda, H.Tsubota*, T.Yamaya**, B-N.sung***,

A.Kagaya, K.Takeshita, H.Yamazaki and T.Shimada

1) $^{40}Ca(\gamma,\pi^+)^{40}K$ by 185 MeV electron beam: Strong π^+ photoproduction leaving states around 0.9, 2.7, 4.4 and 6.1 MeV in ^{40}K are found. Angular distributions of π^+ emission have been studied as an example in fig.1. The paper is in press in Nucl. Phys. A.

2) $^{9}Be(e,\pi^+)^{9}Li$ by $\sim$200 MeV electron beam: Energy distribution of π^+ for strong spin-isospin flip transitions have been studied as shown in fig.2. π^+ angular distributions are also studied.

3) Study of the analogue state of 1.7 MeV state in ^{9}Be: The analogue missing partner in ^{9}B of the first excited state $1/2^+$ at 1.7 MeV in ^{9}Be have been observed at $E_x \sim 0.9$ MeV by the (e,π^+) reaction of 172 MeV (fig.3). This state in ^{9}Be is a single neutron state in s-wave scattering, so the resonance is hardly considered as the usual Brei-Wigner one.

4) Systematics of (γ,π^+) yields with $\sim$200MeV semi-monochromatic

* College of General Education, Tohoku University.

** Department of Physics, Tohoku University

*** Department of Physics, Seoul University, Korea

γ rays by photon difference method: An example of the results is shown in fig.4. Theoretical curves for the quasi-free production can not reproduce the results.

5) Publised papers:

(A) Charge Number Dependence of π^+ Production from Nuclei by 200 MeV Electron. Nucl. Phys. A486(1988)512.
Systematics of (e,π^+) yields with 200 MeV electrons have been studied. The yields is 1/7.5 times of the theory.

(B) Branchin of π^+ in $^{12}C(\gamma,\pi^+)$ Reaction. Nucl. Phys. A486 (1988)526.
Energy and angular distributions of (γ,π^+) have been studied by photon difference method for branching of π^+.

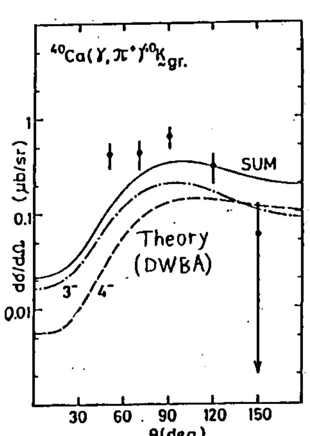

Fig.1.

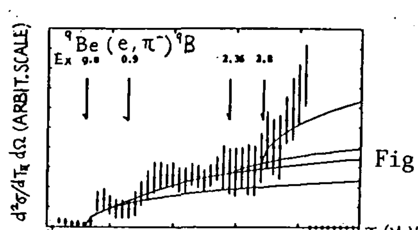

Fig.3.

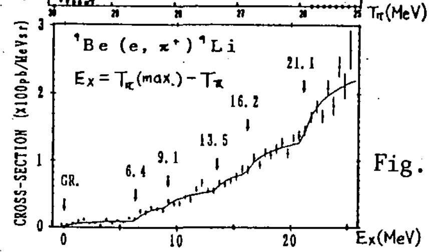

Fig.2.

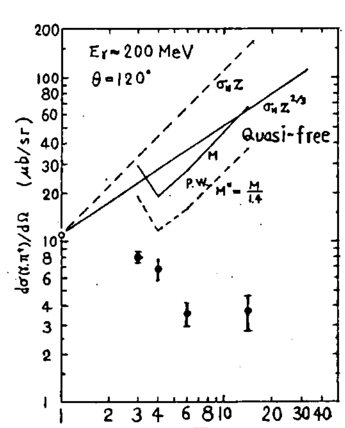

Fig.4.

COINCIDENCE (e,e'p) EXPERIMENTS

Y.Kawazoe*, Y.Kawahara, H.Matsuyama, H.Miyase**, K.Namai, M.Nomura, M.Sugawara, T.Tadokoro, T.Tamae, H.Tsubota**.

The (e,e'p) coincidence cross sections have been measured using the 129 MeV electron beams of high duty cycle (~80%) from the stretcher ring (SSTR). The scattered electrons are momentum-analysed by a magnetic spectrometer at 30°.

^{6}Li(e,e'p)

The coincidence cross sections have been measured at θ_p= 0°, 30° (ϕ_p= 45° and 135°) and 180°, in the excitation energy range between 20 and 25 MeV. The mean value of the momentum transfer was q = 0.33 fm^{-1}. Protons were detected with 1 mm surface-barrier solid-state detectors. A missing energy spectrum of the protons is shown in Fig.1, where p_0 protons(^{6}Li→^{5}He+p) are separated from the continuous part(^{6}Li→ α +p+n).

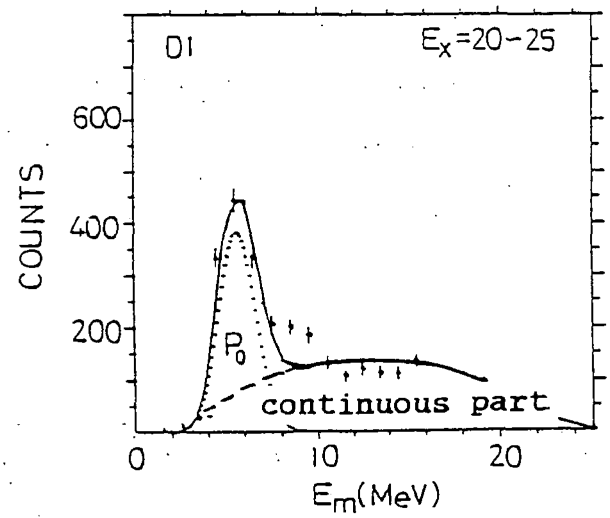

Fig. 1 Missing energy spectrum.

^{16}O(e,e'p_0)

Protons were detected in the giant resonance region by using plastic scintillators at the angles out of the scattering plane. These experiments make possible to derive interference terms of longitudinal and transverse term. The results are reasonable agreement with the ones expected from (γ,p_0) and other (e,e'p_0) data. In this experiment, the reaction target (BeO) are set inside a He-gass bag in order to arrange the proton detectors at angles surrounding the target. This method was adopted to obtain technical information for extending the out-of-plane coincidence experiments into the higher energy region.

---

* Education Center for Information processing, Tohoku Univ.
** College of General Education, Tohoku Univ.

VIII-C-3 C(e,e'n) Experiment

K.Takahisa, T.Saito, S.Suzuki, T.Tohei*,

T.Nakagawa*, Y.Kobayashi* and K.Abe**

We have performed measurements on $^{12}C(e,e'n)$ reaction using a continuous electron beam from the Tohoku University 150-MeV pulse stretcher ring[1] and the first angular distributions of neutrons emitted from the giant resonance of ^{12}C have been succesfully obtained[2].

Each neutron detector consists of an 8" diameter 4" depth NE213 liquid scintillator accompanied by a 5" R1250 photomultiplier tube[3,4]. The scattered electrons were momentum analyzed by a magnetic spectrometer and detected by a combination of multiwire proportional chambers and plastic scintillators.

The scattered electrons were measured at a 30° scattering angle, which corresponds to momentum transfer $q=0.33\ fm^{-1}$, which favors E1 excitation.

The missing energy spectrum is shown in Fig. 1. We plot the missing energy relative to the ^{11}C ground state at 18.7 MeV. The branching ratio of the ^{12}C giant resonance shows that n_0 transitions account for about 80% of decays.

The angular distribution is shown in Fig. 2. We plot the data at 23.5 MeV. The black circles show $(e,e'n_0)$ data. There is some assymmetry of momentum transfer about the anti momentum transfer direction. This is due to multipolarities other than

* Department of Physics, Tohoku University

** College of General Education, Tohoku University

dipole. The solid line is an RPA calculation[5] for energy 22.5 MeV and momentum transfer $q=0.43\ fm^{-1}$. The open circles show $(e,e'p_0)$ data[6]. We can see that the $(e,e'n_0)$ distribution is a little different from that of $(e,e'p_0)$.

References:

1) T.Tamae et al., Nucl. Instr. Meth. A264(1988)173.
2) T.Saito et al., Abst. of 17th INS Internatinal Symposium on Nuclear Physics at Intermediate Energy, Tokyo 1988, p. 84.
3) K.Takahisa et al., Research Report of Laboratory of Nuclear Science 21(1988)145.
4) K.Takahisa et al., Research Report of Laboratory of Nuclear Science 22(1989)1.
5) M.Cavinato et al., Nucl. Phys. A444(1985)13.
6) J.R.Calarco et al., Phys. Lett. 146B(1984)179.

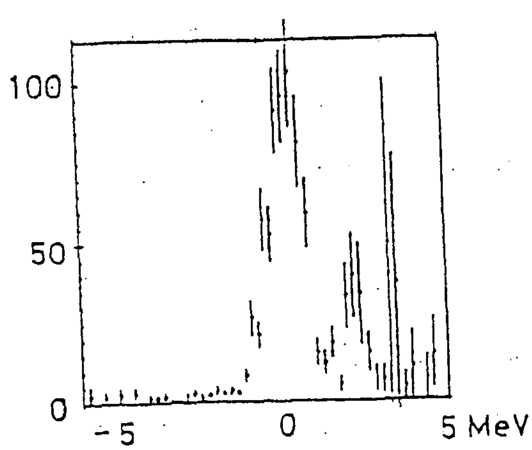

Fig. 1. Missing energy spectrum.

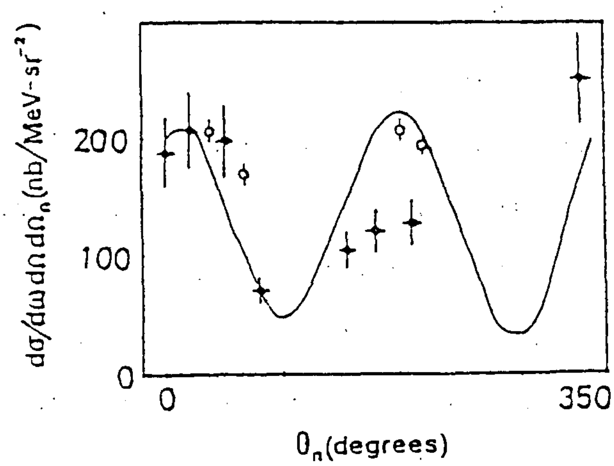

Fig. 2. Angular distribution.

VIII-C-4

Experiments with Tagged Photons below Pion Threshold

A.Bates**, O.Konno, K.Maeda*, D.McLean, I.Nomura, R.Rassool**, T.Suda*, Y.Sugawara, T.Terasawa, M.Thompson**, Y.Torizuka and J.Yokokawa

Photoprotons and photoneutrons from light nuclei have been measured using tagged photons of energies between 24 and 102 MeV. The energy resolution and the intensity of the tagged photons were typically 2.6 MeV and about 10^6/s, respectively.

^{6,7}Li(γ ,p)

Three prominent bumps corresponding to the protons knocked out from the 1p-shell, 1s-shell and quasi-deutron (QD) process have been observed in the proton spectra of both ^{6}Li and ^{7}Li(γ , p) reactions. The ratios of the ^{7}Li to ^{6}Li(γ,p) cross sections for the 1p-shell, 1s-shell and QD protons were 2, 1 and 1.3, respectively. The ratios for the 1p- and 1s-shell protons were well accounted for by the quasi-free knockout (QFK) hypothesis.

The momentum distributions of the 1s-shell protons in the ground states of the ^{6}Li and ^{7}Li nuclei were deduced by assuming QFK. It has been found that the momentum distribution of the 1s-protons in the ^{6,7}Li nuclei coincides with that of the ^{4}He nucleus.

^{4}He(γ ,n)

Above experiment has been made using a liquid helium target. Tagged photon energies covered the giant E1 resonance, where the charge symmetry breaking of the nuclear force has been discussed through a large difference between the (γ ,p) and (γ ,n) cross sections. Our data showed good agreement with the data previously obtained by B.L.Berman *et al.* [1]).

Ref. 1) B.L.Berman *et al.* ; Phys. Rev. **c22** (1980) 2273

---

* College of General Education, Tohoku University
** The University of Melbourne, Parkville, Victoria 3052, Australia

IX. TOKYO INSTITUTE OF TECHNOLOGY

IX-A-1

Mechanism of Electric dipole transitions from broad p-wave neutron resonance in ^{24}Mg

T. Uchiyama, M. Igashira, and H. Kitazawa

Neutron Capture gamma rays from the 84-keV $p_{3/2}$-wave resonance, 266-keV $p_{1/2}$-wave resonance and 431-keV $p_{3/2}$-wave resonance in ^{24}Mg which have large reduced neutron width have been measured with an anti-Compton NaI(Tl) detector, using a time-of-flight technique. Successful extraction of gamma-ray intensities for transitions to low-lying states in ^{25}Mg was performed by an iterative unfolding method in order to deduce partial radiative widths. Also, we made an experimental contrivance separating the kernel of the 266-keV broad resonance from that of the 257-keV overlapping narrow resonance. Radiative widths were obtained for the E1 transitions to the ground ($5/2^+$), 585-keV ($1/2^+$), 975-keV ($3/2^+$), 1965-keV ($5/2^+$), 2564-keV ($1/2^+$) and 2801-keV ($3/2^+$) states, and compared with theoretical calculations based on the valence capture model which has been developed by Lane and Mughabghab. Consequently, we found that in the $p_{3/2}$-wave resonance capture the observed and calculated widths for the transitions to the $1/2^+$ states are in excellent agreement, however the experimental widths for the transitions to the $5/2^+$ states are 20-50% of the theoretical ones. These noteworthy features in the retardation of E1 transition are explained in terms of the renormalized effective charge which depends on the orbital angular momentum for the single-particle component of final bound states, as a result of the coupling of the single-particle transition with the isovector field generated by the giant dipole resonance. Moreover, the non-adiabatic coupled channel calculation using a particle-rotator coupling model was carried out for partial radiative widths of the 266-keV $p_{1/2}$-wave resonance. The calculations reproduced the observed values satisfactorily.